PHYSICAL REVIEW A VOLUME 59, NUMBER 5 MAY 1999

Influence of the pure vibrational dephasing processes on the dip structure in pumped sum-frequency generation spectroscopy

A. A. Villaeys and F. P. Lohner
Institut de Physique et Chimie des Matériaux de Strasbourg, 23, Rue du Loess, 67037 Strasbourg Cedex, France

(Received 14 September 1998)

Recent theoretical analysis of infrared-visible pumped sum-frequency spectroscopy on adsorbed molecules exhibits a dip structure on the frequency dependence of the sum-frequency signal intensity. To get more physical insight into this dip, which has not yet been observed experimentally, we present a unified description capable of handling, on the same footing, steady-state and pulsed experiments. Contrary to previous treatments, this description is valid for any duration of the dephasing times. Therefore, it enables a detailed discussion about the origin of the dip, as well as a determination of the conditions of its observability. These conditions are, in fact, very sensitive to the pure vibrational dephasing processes. In the nonresonant conditions, usually adopted in these experiments for the visible probe beam, the pure electronic dephasing does not affect the dip structure and the underlying dynamics. However, if the visible probe beam becomes resonant with the electronic transition, the pure electronic dephasing introduces a strong asymmetry of the dip.

[S1050-2947(99)00505-3]

PACS number(s): 42.65.Ky, 42.50.Ct

I. INTRODUCTION

Today, a large number of nonlinear optical spectroscopies are currently applied to the studies of the various dynamical processes taking place in material systems. Among the great panel of techniques based on optical nonlinearities, second-order optical processes involving second-harmonic generation (SHG) and sum-frequency generation (SFG) are of special interest to determine the physical properties and the underlying dynamics taking place on the surfaces, interfaces, as well as in the adsorbed systems [1–6].

Among all these spectroscopic methods, infrared-visible sum-frequency generation (IRVSFG) experiments constitute a vibrational spectroscopic method of particular interest to identify the adsorbed species deposited on surfaces, and to study their dynamical evolution. Systems as different as adsorbed molecules [7,8], Langmuir-Blodgett films [9–12], or even the formation of dimers or clusters at surfaces [13] have been the subject of numerous studies.

More recently, by introducing an additional infrared pump beam, it has been possible to study the dynamical processes involving the hot band of the spectra. Here, the molecule initially populated by an infrared pump pulse is ultimately tested by two coincident infrared and visible probe pulses. Due to the possible overlapping of the pulses, the nonlinear process underlying the polarization created on the molecule is really a five-wave mixing process involving the characteristic sequential, self-modulation, and interference terms. From the detailed analysis presented here, we will show that we really have two different contributions of similar magnitude which contribute to the interference terms. They are termed synchronous and asynchronous interference terms because of the ordering of the infrared pump and probe beam interactions. By using this pumped infrared-visible sum-frequency generation (PIRVSFG), the anharmonicity of the Si-H stretch mode of H/Si(111)(1×1) has been determined [14].

For pulsed PIRVSFG experiments, quantities such as the recovery time of the ground-state population of either the Si-H stretch mode of the H/Si(111)(1×1) [14,15] or the C-H stretch mode of the H/C(111)(1×1) [16,17], as well as the vibrational energy relaxation of the C-H stretch mode of methyl thiolate adsorbed on metallic surface [18–20], have been experimentally determined. In a recent theoretical study on surface vibrational infrared-visible sum-frequency generation spectroscopy applied to adsorbed molecules [21], frequency and time dependences of physical observables have been evaluated on the basis of Gaussian light pulses whose durations are supposed to be longer than any dephasing times. Recovery time profiles and time dependence of the transient SFG signal have been evaluated for experimental situations where the infrared probe beam was resonant with either the first or the second vibrational transition.

However, some information can yet be extracted from the frequency dependence of the second-order and fourth-order polarization terms, which have been determined in the steady-state regime. Both terms are required since, for this type of experiment, the phase-matching conditions cannot disentangle second-order and fourth-order contributions, even when the three pump and probe beams have different orientations. A peculiar feature of these variations is the observation of a dip in the frequency dependence of the fourth-order polarization term. At present, this dip has not been observed experimentally. It is the goal of the present work to get some physical insight into this dip, and to define the conditions for its observability.

The paper is organized as follows. In Sec. II, we introduce the model for the adsorbed system, as well as the characteristics and geometry of the pulsed and probe beams used in this experiment. With the present description, steady-state and pulsed situations can be handled on the same footing. Notice that due to the combination of second-order and fourth-order terms contributing to the pumped sum-frequency signal, we cannot define a nonlinear optical susceptibility. For this reason, we will discuss the physical insights in terms of the nonlinear polarization. Section III is

1050-2947/99/59(5)/3926(15)/$15.00

devoted to the general description of the dynamics involved in the five-wave mixing process. Besides the existence of the sequential and self-modulation terms, we will establish that the additional interference term results from two different contributions comparable in magnitude. They are associated with synchronous and asynchronous contributions of the interference term taking place between the pump and probe beams. In Sec. IV, we focus on the frequency dependence of the various contributions to the five-wave mixing process only, and analyze the influence of the pure vibrational processes in the frequency region where the dip is located. Finally, in Sec. V, we discuss the conditions of observability of the dip in pumped sum-frequency generation experiment subject to electronic and vibrational dephasing. As expected, due to the nonresonant conditions for the visible probe beam, it will be shown that the pure electronic dephasing does not affect the frequency structure of the dip.

II. DESCRIPTION OF THE ADSORBED SYSTEM AND FIELDS

The dynamical evolution of a molecular system undergoing relaxation and dephasing processes, and interacting with one pump beam and two probe beams, satisfies the Liouville equation given by

$$\frac{\partial \rho(t)}{\partial t} = -\frac{i}{\hbar}[L_0 + L_V(t)]\rho(t) - \Gamma \rho(t), \tag{2.1}$$

where $\rho(t)$ represents its density matrix and Γ is the damping operator involving the relaxation and dephasing constants accounting for its surrounding. All of them will be explicitly given in the next section since they will be required for the evaluation of the dynamics. To avoid the well-known artificial discrepancy encountered in the evaluation of four-wave-mixing processes like Rayleigh-type optical mixing and pump-probe absorption applied to homogeneously broadened lines [22–24], we introduce all the constants and take their limiting values after performing the time integration. Here, special attention will be paid to the pure vibrational dephasing occurring in the vibrational structure of the ground electronic configuration and induced by the surface. Notice that the pure dephasing constant $\Gamma_{ij}^{(d)}$ is related to the dephasing constant by the relation $\Gamma_{ijij} = \frac{1}{2}[\Gamma_{iiii} + \Gamma_{jjjj}] + \Gamma_{ij}^{(d)}$. In addition, L_0 is the Liouvillian associated to the zero-order Hamiltonian H_0, and $L_V(t)$ is the Liouville operator for the interaction $V(t)$ between the adsorbed system and the radiation fields.

For our purpose, a convenient model of the adsorbed system can be made of two electronic configurations, the ground and the first excited configurations, and of one stretch vibrational mode which is the bonding mode between the surface and the adsorbed species, say C-H or Si-H in most of the cited experiments. While only the first three vibrational states of the ground configuration are required for the dynamics of the five-wave mixing, we do not introduce the vibrationally excited states in the excited electronic configuration because the visible beam is always nonresonant with the electronic transition. With the usual conditions adopted in this type of experiment, the sum of the infrared and visible field frequencies is always much lower than the electronic transition frequency. Therefore, the energy mismatch due to these nonresonant conditions is always greater than the vibrational energy of the level which can be involved in the dynamical process. For this reason, the vibrational excited states of the excited electronic configuration do not influence the frequency dependence of the absorption spectrum. This is known as the Placzek approximation [25], and has been extensively used in the literature. The model is introduced in Fig. 1. Levels 1 to 3 are the electronic and vibrational levels of the ground electronic configuration and level 4 corresponds to the excited electronic configuration vibrationally unexcited. The relevant transition dipole moments are shown in the figure. To avoid additional contributions in the detected signal, the optical beams are collimated in three different directions. In addition, the infrared pump beam has a fixed frequency and is resonant with the first vibrational transition ω_{21}, while the infrared probe beam is scanned around the second vibrational transition frequency ω_{32}, which differs from ω_{21} because of anharmonicity. Within the dipole approximation and the rotating-wave approximation valid for the infrared pump and probe fields only, $V(t)$ takes the form

$$\begin{aligned} V_{mn}(t) = -\langle m|\vec{\mu}|n\rangle \cdot \Big[& \vec{E}(\sigma_{mn}\omega_{\mathrm{IR}}) e^{-i\sigma_{mn}(\omega_{\mathrm{IR}}t - \vec{k}_{\mathrm{IR}}\cdot\vec{r})} \mathcal{L}_{\mathrm{IR}}(t) \\ & + \vec{E}(\sigma_{mn}\omega_{\mathrm{ir}}) e^{-i\sigma_{mn}(\omega_{\mathrm{ir}}t - \vec{k}_{\mathrm{ir}}\cdot\vec{r})} \mathcal{L}_{\mathrm{ir}}(t) \\ & + \sum_{s=\pm 1} \vec{E}(s\omega_{\mathrm{vis}}) e^{-is(\omega_{\mathrm{vis}}t - \vec{k}_{\mathrm{vis}}\cdot\vec{r})} \mathcal{L}_{\mathrm{vis}}(t) \Big], \end{aligned} \tag{2.2}$$

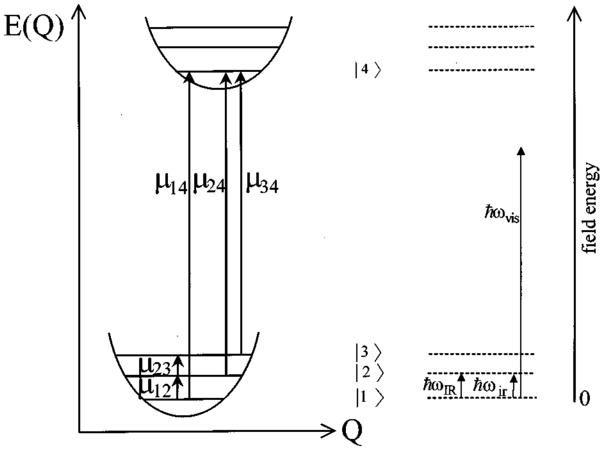

FIG. 1. Representation of the model introduced for the adsorbed system. In the left part of the figure, Q is the bonding coordinate between the adsorbed system and the surface. The two parabolas stand for the ground and first excited electronic configurations. The vibronic levels $|1\rangle = |g,0\rangle$, $|2\rangle = |g,1\rangle$, $|3\rangle = |g,2\rangle$, and $|4\rangle = |e,0\rangle$ are shown in the figure. The notations g and e stand for the electronic configuration and 0,1,2,... for the vibrational quantum number. Their corresponding vibrational energies are different because of anharmonicity and are given by $\omega_{21} = 2838\,\mathrm{cm}^{-1}$ and $\omega_{32} = 2736\,\mathrm{cm}^{-1}$. The transition electronic energy is set equal to $\omega_{41} = 30\,000\,\mathrm{cm}^{-1}$. The dipole moments are chosen real and their modulli correspond to $\mu_{12} = \mu_{14} = \mu_{24} = \mu_{34}$, while $\mu_{23} = 1.5\,\mu_{12}$. The dephasing constants are given by $\Gamma_{1313} = 30\,\mathrm{cm}^{-1}$, $\Gamma_{1414} = 30\,\mathrm{cm}^{-1}$, $\Gamma_{2323} = 15.5\,\mathrm{cm}^{-1}$, $\Gamma_{2424} = 40\,\mathrm{cm}^{-1}$, and $\Gamma_{3434} = 30\,\mathrm{cm}^{-1}$. On the right part of the figure, we represent the energies of the infrared pump and visible probe fields used in this experiment.

where ω_p, $\vec{k}_p$, and $\mathcal{L}_p(t)$ are the frequencies, wave vectors, and laser pulse shapes of the infrared pump ($p=\mathrm{IR}$), infrared probe ($p=\mathrm{ir}$), and visible probe ($p=\mathrm{vis}$) pulses. Also, the symbol σ_{mn} is equal to $+1$ or -1, depending on whether the energy gap between the states $|m\rangle$ and $|n\rangle$, corresponding to (E_m-E_n), is positive or negative, respectively. For the sake of convenience, we shall choose

$$\mathcal{L}_j(t)=e^{-\gamma_j|\overline{t_j}-t|}=e^{-\gamma_j(t-\vec{t}_j)}H(t-\overline{t_j})+e^{\gamma_j(t-\overline{t_j})}\overline{H}(\overline{t_j}-t), \tag{2.3}$$

where $\overline{t_j}$ represents the pumping or probing times and $T_j=\gamma_j^{-1}$ is the corresponding pumping or probing pulse duration, depending on the nature of the field j. Also, $H(t)$ stands for the Heaviside function with the additional notation, $\overline{H}(t)=1-H(-t)$. It has to be mentioned that the introduction of the previous line shape enables a unified description of the steady-state and time-resolved situations, depending on whether the pulse durations are longer or shorter with respect to the time constants of the material system.

III. DYNAMICAL EVOLUTION INVOLVED IN A FIVE-WAVE-MIXING EXPERIMENT

In a pumped SFG experiment, the wave vectors of the infrared pump beam do not contribute to the phase-matching condition because their sum cancels. Therefore, in the direction of the phase-matched SFG signal, we will necessarily have a three-wave-mixing background which contributes to the five-wave-mixing signal. As a consequence, the corresponding polarization is given by

$$\vec{P}(t)=\vec{P}^{(2)}(\vec{k}_{\mathrm{SF}},t)+\vec{P}^{(4)}(\vec{k}_{\mathrm{SF}},t). \tag{3.1}$$

The second-order contribution is obtained from the perturbational expansion of Eq. (2.1) with respect to the interaction $V(t)$. It can be written in terms of the Liouvillian evolution operator defined by $G(t-t')=\exp\{[-(i/\hbar)L_0-\Gamma](t-t')\}$. For a system interacting first with the field I and next with the field J, it takes the form

$$\begin{aligned}\vec{P}^{(2)}(I,J;\vec{k}_{\mathrm{SF}},t)=\mathrm{Tr}\Bigg[\left(-\frac{i}{\hbar}\right)^2\int_{-\infty}^{t}dt_2\int_{-\infty}^{t_2}dt_1G(t-t_2)\\ \times L_{V(J)}(t_2)G(t_2-t_1)L_{V(I)}(t_1)\rho(-\infty)\vec{\mu}\Bigg],\end{aligned} \tag{3.2}$$

where the symbol $L_{V(Q)}$ stands for the Liouvillian involving the interaction with the field Q only. In addition, the various matrix elements can be expressed as

$$\begin{aligned}G_{mnmn}(t'-t'')&=e^{-i(\omega_{mn}-i\Gamma_{mn})(t'-t'')},\\ L_{V\,mnpq}(t)&=V_{mp}(t)\,\delta_{qn}-V_{qn}(t)\,\delta_{mp}.\end{aligned} \tag{3.3}$$

This is all that we need to calculate the contributions associated to the second-order background contributions. With our previous assumptions, only the pathways schematically represented by

ρ	G	L_V	G	L_V	ρ_i
41	4141	4121	2121	2111	11
24	2424	2421			

contribute efficiently to the $\vec{k}_{\mathrm{SF}}=\vec{k}_{\mathrm{ir}}+\vec{k}_{\mathrm{vis}}$ component of the polarization. If we note that the contribution associated to any pathway η can be formally written as

$$\begin{aligned}\overrightarrow{CP}_{\eta}^{(2)}(I,J;\vec{k}_{\mathrm{SF}},t)=\left(-\frac{i}{\hbar}\right)^2\vec{S}_{\eta}^{(2)}e^{s_{\eta}^{(2)}t}e^{i\vec{k}_{\mathrm{SF}}\cdot\vec{r}}\\ \times\int_{-\infty}^{t}dt_2e^{B_{\eta}^{(2)}t_2}e^{-\gamma_j|t_2-\overline{t_j}|}\\ \times\int_{-\infty}^{t_2}dt_1e^{A_{\eta}^{(2)}t_1}e^{-\gamma_i|t_1-\overline{t_i}|},\end{aligned} \tag{3.4}$$

the second-order polarization, in the direction $\vec{k}_{\mathrm{SF}}$, is given by

$$\begin{aligned}\vec{P}^{(2)}(\vec{k}_{\mathrm{SF}},t)&=\sum_{\eta=1}^{2}\overrightarrow{CP}_{\eta}^{(2)}(I,J;\vec{k}_{\mathrm{SF}},t)\\ &=\sum_{\eta=1}^{2}\vec{S}_{\eta}^{(2)}e^{s_{\eta}^{(2)}t}e^{i\vec{k}_{\mathrm{SF}}\cdot\vec{r}}\Bigg[\sum_{\beta=1}^{7}H(t-\tau_{\beta\eta}^{>})D_{\beta\eta}^{>}e^{d_{\beta\eta}^{>}t}\\ &\quad+\overline{H}(\tau_{1\eta}^{<}-t)D_{1\eta}^{<}e^{d_{1\eta}^{<}t}\\ &\quad+\sum_{\beta=1}^{6}H(t-\tau_{1,\beta\eta}^{\times})\overline{H}(\tau_{2,\beta\eta}^{\times}-t)D_{\beta\eta}^{\times}e^{d_{\beta\eta}^{\times}t}\Bigg],\end{aligned} \tag{3.5}$$

where the constants of integration are given in Appendix A. Notice that this polarization contribution $\vec{P}^{(2)}(\vec{k}_{\mathrm{SF}},t)$ is expressed in terms of the constants resulting from the second time integration constants alone, as shown in Appendix A. However, a rapid inspection of these quantities clearly shows that they are functions of the first time integration constants. This is why they are listed in Appendix A. For the sake of simplicity, we have introduced the notations $\vec{E}(\omega_p)=\vec{E}_p$ and $\vec{E}(-\omega_p)=\vec{E}_p^*$ for $p=\mathrm{IR}$, ir, and vis. Moreover, the various constants of the pathways 1 and 2 taken by order from the top to the bottom are given in Table I. Similarly, with the same assumptions, the fourth-order contribution to the polarization, which can be written as

$$\begin{aligned}&\vec{P}^{(4)}(I,J,K,L;\vec{k}_{\mathrm{SF}},t)\\ &\quad=\mathrm{Tr}\Bigg[\left(-\frac{i}{\hbar}\right)^4\int_{-\infty}^{t}dt_4\int_{-\infty}^{t_4}dt_3\int_{-\infty}^{t_3}dt_2\int_{-\infty}^{t_2}dt_1\\ &\qquad\times G(t-t_4)L_{V(L)}(t_4)G(t_4-t_3)L_{V(K)}(t_3)\\ &\qquad\times G(t_3-t_2)L_{V(J)}(t_2)G(t_2-t_1)L_{V(I)}(t_1)\rho(-\infty)\vec{\mu}\Bigg],\end{aligned} \tag{3.6}$$

is associated with the pathways

TABLE I. Constants associated with the pathways required for the calculations of $\vec{P}^{(2)}(I,J;\vec{k}_{\mathrm{SF}},t)$.

$\vec{S}_1^{(2)}=-\frac{\vec{\mu}_{14}}{\hbar^2}\vec{\mu}_{42}\cdot\vec{E}_{\mathrm{vis}}\vec{\mu}_{21}\cdot\vec{E}_{\mathrm{ir}}$	$A_1^{(2)}=i\omega_{21}+\Gamma_{2121}-i\omega_{\mathrm{ir}}$
$s_1^{(2)}=-i\omega_{41}-\Gamma_{4141}$	$B_1^{(2)}=i\omega_{41}+\Gamma_{4141}-i\omega_{\mathrm{vis}}-i\omega_{21}-\Gamma_{2121}$
$\vec{S}_2^{(2)}=\frac{\vec{\mu}_{42}}{\hbar^2}\vec{\mu}_{14}\cdot\vec{E}_{\mathrm{vis}}\vec{\mu}_{21}\cdot\vec{E}_{\mathrm{ir}}$	$A_2^{(2)}=i\omega_{21}+\Gamma_{2121}-i\omega_{\mathrm{ir}}$
$s_2^{(2)}=i\omega_{42}-\Gamma_{2424}$	$B_2^{(2)}=-i\omega_{42}+\Gamma_{2424}+i\omega_{\mathrm{vis}}-i\omega_{21}-\Gamma_{2121}$

ρ	G	L_V	G	L_V	G	L_V	G	L_V	ρ_i
24	2424	2421	2121	2111	1111	1112	1212	1211	11
41	4141	4121							
24	2424	2421	2121	2122	2222	2212			
41	4141	4121							
34	3434	3432	3232	3222					
42	4242	4232							
24	2424	2421	2121	2111	1122				
41	4141	4121							
41	4141	4121	2121	2131	3131	3121	2121	2111	
42	4242	4232	3232	3231					
34	3434	3432							
41	4141	4121	2121	2111	1111	1121			
24	2424	2421							
42	4242	4232	3232	3222	2222	2221			
34	3434	3432							
41	4141	4121	2121	2122					
24	2424	2421							
41	4141	4121	2121	2111	1122				
24	2424	2421							

Here, contrary to the second-order contribution where only coherence is involved, the evolution of the populations, as well as the transfer of the populations, contribute to the various pathways. For this reason, their corresponding evolution Liouvillians $G_{mmnn}(t'-t'')$ need to be evaluated [26]. Their formal expressions can be expressed as

$$G_{mmnn}(t'-t'')=\sum_{\alpha=1}^{4}\langle\langle mm|\alpha\alpha\rangle\rangle\langle\langle\alpha\alpha|nn\rangle\rangle e^{-\overline{\Gamma}_{\alpha}(t'-t'')}. \tag{3.7}$$

We still have to evaluate the eigenvalues and overlappings contributing to the spectral decomposition of the Green function $G_{mmnn}(t'-t'')$. If we remember that the coherences are diagonal in the Liouvillian space, we just need to diagonalize the population Liouvillian space. We have

$$\frac{\partial}{\partial t}\rho_{ii}(t)=\sum_{j} M_{iijj}\rho_{jj}(t), \tag{3.8}$$

where, for our model, the matrix M corresponds to

$$M=\begin{pmatrix} -\Gamma_{1111} & -\Gamma_{1122} & -\Gamma_{1133} & -\Gamma_{1144}\\ -\Gamma_{2211} & -\Gamma_{2222} & -\Gamma_{2233} & -\Gamma_{2244}\\ 0 & 0 & -\Gamma_{3333} & -\Gamma_{3344}\\ 0 & 0 & 0 & -\Gamma_{4444}\end{pmatrix}. \tag{3.9}$$

The eigenvalues $\overline{\Gamma}_{\alpha}$ and overlappings $\langle\langle mm|\alpha\alpha\rangle\rangle$ are obtained from the Laplace transform of the previous equation (3.8). It gives

$$\hat{\rho}(p)=[pI-M]^{-1}\rho(0), \tag{3.10}$$

so that

$$\rho(t)=\int_{-\infty+i\epsilon}^{+\infty+i\epsilon}dt\, e^{pt}[pI-M]^{-1}\rho(0)\equiv G(t)\rho(0). \tag{3.11}$$

From the inverse of the matrix M, and the introduction of the closure relation $\Gamma_{pppp}=-\Sigma_{q\neq p}\Gamma_{qqpp}$, the eigenvalues are easily obtained:

$$\overline{\Gamma}_1=0,\quad \overline{\Gamma}_2=\Gamma_{1111}+\Gamma_{2222},\quad \overline{\Gamma}_3=\Gamma_{3333},\quad \overline{\Gamma}_4=\Gamma_{4444}. \tag{3.12}$$

Next, using the time translation invariance, the matrix elements of $G(t_i-t_j)$ are straightforwardly deduced. They are given by the following expressions:

$$\begin{aligned}
G_{1111}(t_i-t_j)&=\frac{\Gamma_{1111}e^{-(\Gamma_{1111}+\Gamma_{2222})(t_i-t_j)}+\Gamma_{2222}}{\Gamma_{1111}+\Gamma_{2222}},\\
G_{1122}(t_i-t_j)&=\frac{-\Gamma_{2222}e^{-(\Gamma_{1111}+\Gamma_{2222})(t_i-t_j)}+\Gamma_{2222}}{\Gamma_{1111}+\Gamma_{2222}},\\
G_{2211}(t_i-t_j)&=\frac{-\Gamma_{1111}e^{-(\Gamma_{1111}+\Gamma_{2222})(t_i-t_j)}+\Gamma_{1111}}{\Gamma_{1111}+\Gamma_{2222}},\\
G_{2222}(t_i-t_j)&=\frac{\Gamma_{2222}e^{-(\Gamma_{1111}+\Gamma_{2222})(t_i-t_j)}+\Gamma_{1111}}{\Gamma_{1111}+\Gamma_{2222}}.
\end{aligned} \tag{3.13}$$

We must bear in mind that, for the pumped sum-frequency generation experiment considered here, only these quantities describing the evolution or the transfer of the populations are required. From the previous expressions, the contribution of any pathway η to the polarization can be evaluated. For an (I,J,K,L) combination of fields, it is given by the formal expression

$$\begin{aligned}
\overrightarrow{CP}_{\eta}^{(4)}&(I,J,K,L;\vec{k}_{\mathrm{SF}},t)\\
&=\left(-\frac{i}{\hbar}\right)^4\vec{S}_{\eta}^{(4)}e^{s_{\eta}^{(4)}t}\int_{-\infty}^{t}dt_4e^{D_{\eta}^{(4)}t_4}e^{-\gamma_1|t_4-\overline{t_l}|}\\
&\quad\times\int_{-\infty}^{t_4}dt_3e^{C_{\eta}^{(4)}t_3}e^{-\gamma_k|t_3-\overline{t_k}|}\int_{-\infty}^{t_3}dt_2e^{B_{\eta}^{(4)}t_2}e^{-\gamma_j|t_2-\overline{t_j}|}\\
&\quad\times\int_{-\infty}^{t_2}dt_1e^{A_{\eta}^{(4)}t_1}e^{-\gamma_i|t_1-\overline{t_i}|},
\end{aligned} \tag{3.14}$$

TABLE II. Constants associated with the pathways participating in the calculation of $\vec{P}^{(4)}(I,J,K,L;\vec{k}_{\mathrm{SF}},t)$. Notice that the quantity $X^{(4)}_{p.[1,2]}$ is given by the expression involving the left part of the brackets for index 1, and the right part of the brackets for index 2. In addition, we have introduced the notation $\Gamma_{1111}+\Gamma_{2222}=\Gamma_{\mathrm{tot}}$.

$\vec{S}^{(4)}_{1.[1,2]}=-\dfrac{[\Gamma_{1111},\Gamma_{2222}]\vec{\mu}_{42}\vec{\mu}_{14}\cdot\vec{E}_L\vec{\mu}_{21}\cdot\vec{E}_K\vec{\mu}_{21}\cdot\vec{E}_J\vec{\mu}_{12}\cdot\vec{E}_I^\star}{\hbar^4\Gamma_{\mathrm{tot}}}$ $s^{(4)}_{1.[1,2]}=i\omega_{42}-\Gamma_{4242}$	$A^{(4)}_{1.[1,2]}=i\omega_I-i\omega_{21}+\Gamma_{2121}$ $B^{(4)}_{1.[1,2]}=-i\omega_J+i\omega_{21}+[\Gamma_{\mathrm{tot}}-\Gamma_{2121},-\Gamma_{2121}]$ $C^{(4)}_{1.[1,2]}=-i\omega_K+i\omega_{21}+[\Gamma_{2121}-\Gamma_{\mathrm{tot}},\Gamma_{2121}]$ $D^{(4)}_{1.[1,2]}=-i\omega_L-i\omega_{41}+\Gamma_{4242}-\Gamma_{2121}$
$\vec{S}^{(4)}_{2.[1,2]}=\dfrac{[\Gamma_{1111},\Gamma_{2222}]\vec{\mu}_{14}\vec{\mu}_{42}\cdot\vec{E}_L\vec{\mu}_{21}\cdot\vec{E}_K\vec{\mu}_{21}\cdot\vec{E}_J\vec{\mu}_{12}\cdot\vec{E}_I^\star}{\hbar^4\Gamma_{\mathrm{tot}}}$ $s^{(4)}_{2.[1,2]}=-i\omega_{41}-\Gamma_{4141}$	$A^{(4)}_{2.[1,2]}=i\omega_I-i\omega_{21}+\Gamma_{2121}$ $B^{(4)}_{2.[1,2]}=-i\omega_J+i\omega_{21}+[\Gamma_{\mathrm{tot}}-\Gamma_{2121},-\Gamma_{2121}]$ $C^{(4)}_{2.[1,2]}=-i\omega_K+i\omega_{21}+[\Gamma_{2121}-\Gamma_{\mathrm{tot}},\Gamma_{2121}]$ $D^{(4)}_{2.[1,2]}=-i\omega_L+i\omega_{42}+\Gamma_{4141}-\Gamma_{2121}$
$\vec{S}^{(4)}_{3.[1,2]}=-\dfrac{[\Gamma_{2222},\Gamma_{1111}]\vec{\mu}_{42}\vec{\mu}_{14}\cdot\vec{E}_L\vec{\mu}_{21}\cdot\vec{E}_K\vec{\mu}_{21}\cdot\vec{E}_J\vec{\mu}_{12}\cdot\vec{E}_I^\star}{\hbar^4\Gamma_{\mathrm{tot}}}$ $s^{(4)}_{3.[1,2]}=i\omega_{42}-\Gamma_{4242}$	$A^{(4)}_{3.[1,2]}=i\omega_I-i\omega_{21}+\Gamma_{2121}$ $B^{(4)}_{3.[1,2]}=-i\omega_J+i\omega_{21}+[\Gamma_{\mathrm{tot}}-\Gamma_{2121},-\Gamma_{2121}]$ $C^{(4)}_{3.[1,2]}=-i\omega_K+i\omega_{21}+[\Gamma_{2121}-\Gamma_{\mathrm{tot}},\Gamma_{2121}]$ $D^{(4)}_{3.[1,2]}=-i\omega_L-i\omega_{41}+\Gamma_{4242}-\Gamma_{2121}$
$\vec{S}^{(4)}_{4.[1,2]}=\dfrac{[\Gamma_{2222},\Gamma_{1111}]\vec{\mu}_{14}\vec{\mu}_{42}\cdot\vec{E}_L\vec{\mu}_{21}\cdot\vec{E}_K\vec{\mu}_{21}\cdot\vec{E}_J\vec{\mu}_{12}\cdot\vec{E}_I^\star}{\hbar^4\Gamma_{\mathrm{tot}}}$ $s^{(4)}_{4.[1,2]}=-i\omega_{41}-\Gamma_{4141}$	$A^{(4)}_{4.[1,2]}=i\omega_I-i\omega_{21}+\Gamma_{2121}$ $B^{(4)}_{4.[1,2]}=-i\omega_J+i\omega_{21}+[\Gamma_{\mathrm{tot}}-\Gamma_{2121},-\Gamma_{2121}]$ $C^{(4)}_{4.[1,2]}=-i\omega_K+i\omega_{21}+[\Gamma_{2121}-\Gamma_{\mathrm{tot}},\Gamma_{2121}]$ $D^{(4)}_{4.[1,2]}=-i\omega_L+i\omega_{42}+\Gamma_{4141}-\Gamma_{2121}$
$\vec{S}^{(4)}_{5.[1,2]}=\dfrac{[\Gamma_{2222},\Gamma_{1111}]\vec{\mu}_{43}\vec{\mu}_{24}\cdot\vec{E}_L\vec{\mu}_{32}\cdot\vec{E}_K\vec{\mu}_{21}\cdot\vec{E}_J\vec{\mu}_{12}\cdot\vec{E}_I^\star}{\hbar^4\Gamma_{\mathrm{tot}}}$ $s^{(4)}_{5.[1,2]}=i\omega_{43}-\Gamma_{4343}$	$A^{(4)}_{5.[1,2]}=i\omega_I-i\omega_{21}+\Gamma_{2121}$ $B^{(4)}_{5.[1,2]}=-i\omega_J+i\omega_{21}+[\Gamma_{\mathrm{tot}}-\Gamma_{2121},-\Gamma_{2121}]$ $C^{(4)}_{5.[1,2]}=-i\omega_K+i\omega_{32}+[\Gamma_{3232}-\Gamma_{\mathrm{tot}},\Gamma_{3232}]$ $D^{(4)}_{5.[1,2]}=-i\omega_L-i\omega_{42}+\Gamma_{4343}-\Gamma_{3232}$
$\vec{S}^{(4)}_{6.[1,2]}=-\dfrac{[\Gamma_{2222},\Gamma_{1111}]\vec{\mu}_{24}\vec{\mu}_{43}\cdot\vec{E}_L\vec{\mu}_{32}\cdot\vec{E}_K\vec{\mu}_{21}\cdot\vec{E}_J\vec{\mu}_{12}\cdot\vec{E}_I^\star}{\hbar^4\Gamma_{\mathrm{tot}}}$ $s^{(4)}_{6.[1,2]}=-i\omega_{42}-\Gamma_{4242}$	$A^{(4)}_{6.[1,2]}=i\omega_I-i\omega_{21}+\Gamma_{2121}$ $B^{(4)}_{6.[1,2]}=-i\omega_J+i\omega_{21}+[\Gamma_{\mathrm{tot}}-\Gamma_{2121},-\Gamma_{2121}]$ $C^{(4)}_{6.[1,2]}=-i\omega_K+i\omega_{32}+[\Gamma_{3232}-\Gamma_{\mathrm{tot}},\Gamma_{3232}]$ $D^{(4)}_{6.[1,2]}=-i\omega_L+i\omega_{43}+\Gamma_{4242}-\Gamma_{3232}$
$\vec{S}^{(4)}_{7.[1,2]}=\dfrac{[-\Gamma_{2222},\Gamma_{2222}]\vec{\mu}_{42}\vec{\mu}_{14}\cdot\vec{E}_L\vec{\mu}_{21}\cdot\vec{E}_K\vec{\mu}_{21}\cdot\vec{E}_J\vec{\mu}_{12}\cdot\vec{E}_I^\star}{\hbar^4\Gamma_{\mathrm{tot}}}$ $s^{(4)}_{7.[1,2]}=i\omega_{42}-\Gamma_{4242}$	$A^{(4)}_{7.[1,2]}=i\omega_I-i\omega_{21}+\Gamma_{2121}$ $B^{(4)}_{7.[1,2]}=-i\omega_J+i\omega_{21}+[\Gamma_{\mathrm{tot}}-\Gamma_{2121},-\Gamma_{2121}]$ $C^{(4)}_{7.[1,2]}=-i\omega_K+i\omega_{21}+[\Gamma_{2121}-\Gamma_{\mathrm{tot}},\Gamma_{2121}]$ $D^{(4)}_{7.[1,2]}=-i\omega_L-i\omega_{41}+\Gamma_{4242}-\Gamma_{2121}$
$\vec{S}^{(4)}_{8.[1,2]}=\dfrac{[\Gamma_{2222},-\Gamma_{2222}]\vec{\mu}_{14}\vec{\mu}_{42}\cdot\vec{E}_L\vec{\mu}_{21}\cdot\vec{E}_K\vec{\mu}_{21}\cdot\vec{E}_J\vec{\mu}_{12}\cdot\vec{E}_I^\star}{\hbar^4\Gamma_{\mathrm{tot}}}$ $s^{(4)}_{8.[1,2]}=-i\omega_{41}-\Gamma_{4141}$	$A^{(4)}_{8.[1,2]}=i\omega_I-i\omega_{21}+\Gamma_{2121}$ $B^{(4)}_{8.[1,2]}=-i\omega_J+i\omega_{21}+[\Gamma_{\mathrm{tot}}-\Gamma_{2121},-\Gamma_{2121}]$ $C^{(4)}_{8.[1,2]}=-i\omega_K+i\omega_{21}+[\Gamma_{2121}-\Gamma_{\mathrm{tot}},\Gamma_{2121}]$

TABLE II. (*Continued*).

	$D^{(4)}_{8.[1,2]}=-i\omega_L+i\omega_{42}+\Gamma_{4141}-\Gamma_{2121}$
$\vec{S}^{(4)}_9=\frac{\vec{\mu}_{14}\vec{\mu}_{42}\cdot\vec{E}_L\vec{\mu}_{23}\cdot\vec{E}^{\star}_K\vec{\mu}_{32}\cdot\vec{E}_J\vec{\mu}_{21}\cdot\vec{E}_I}{\hbar^4}$ $s^{(4)}_9=-i\omega_{41}-\Gamma_{4141}$	$A^{(4)}_9=-i\omega_I+i\omega_{21}+\Gamma_{2121}$ $B^{(4)}_9=-i\omega_J+i\omega_{32}+\Gamma_{3131}-\Gamma_{2121}$ $C^{(4)}_9=i\omega_K-i\omega_{32}-\Gamma_{3131}+\Gamma_{2121}$ $D^{(4)}_9=-i\omega_L+i\omega_{42}+\Gamma_{4141}-\Gamma_{2121}$
$\vec{S}^{(4)}_{10}=-\frac{\vec{\mu}_{24}\vec{\mu}_{43}\cdot\vec{E}_L\vec{\mu}_{12}\cdot\vec{E}^{\star}_K\vec{\mu}_{32}\cdot\vec{E}_J\vec{\mu}_{21}\cdot\vec{E}_I}{\hbar^4}$ $s^{(4)}_{10}=-i\omega_{42}-\Gamma_{4242}$	$A^{(4)}_{10}=-i\omega_I+i\omega_{21}+\Gamma_{2121}$ $B^{(4)}_{10}=-i\omega_J+i\omega_{32}+\Gamma_{3131}-\Gamma_{2121}$ $C^{(4)}_{10}=i\omega_K-i\omega_{21}+\Gamma_{3232}-\Gamma_{3131}$ $D^{(4)}_{10}=-i\omega_L+i\omega_{43}+\Gamma_{4242}-\Gamma_{3232}$
$\vec{S}^{(4)}_{11}=\frac{\vec{\mu}_{43}\vec{\mu}_{24}\cdot\vec{E}_L\vec{\mu}_{12}\cdot\vec{E}^{\star}_K\vec{\mu}_{32}\cdot\vec{E}_J\vec{\mu}_{21}\cdot\vec{E}_I}{\hbar^4}$ $s^{(4)}_{11}=i\omega_{43}-\Gamma_{4343}$	$A^{(4)}_{11}=-i\omega_I+i\omega_{21}+\Gamma_{2121}$ $B^{(4)}_{11}=-i\omega_J+i\omega_{32}+\Gamma_{3131}-\Gamma_{2121}$ $C^{(4)}_{11}=i\omega_K-i\omega_{21}+\Gamma_{3232}-\Gamma_{3131}$ $D^{(4)}_{11}=-i\omega_L-i\omega_{42}+\Gamma_{4343}-\Gamma_{3232}$
$\vec{S}^{(4)}_{12.[1,2]}=\frac{[\Gamma_{1111},\Gamma_{2222}]\vec{\mu}_{14}\vec{\mu}_{42}\cdot\vec{E}_L\vec{\mu}_{21}\cdot\vec{E}_K\vec{\mu}_{12}\cdot\vec{E}^{\star}_J\vec{\mu}_{21}\cdot\vec{E}_I}{\hbar^4\Gamma_{\text{tot}}}$ $s^{(4)}_{12.[1,2]}=-i\omega_{41}-\Gamma_{4141}$	$A^{(4)}_{12.[1,2]}=-i\omega_I+i\omega_{21}+\Gamma_{2121}$ $B^{(4)}_{12.[1,2]}=i\omega_J-i\omega_{21}+[\Gamma_{\text{tot}}-\Gamma_{2121},-\Gamma_{2121}]$ $C^{(4)}_{12.[1,2]}=-i\omega_K+i\omega_{21}+[\Gamma_{2121}-\Gamma_{\text{tot}},\Gamma_{2121}]$ $D^{(4)}_{12.[1,2]}=-i\omega_L+i\omega_{42}+\Gamma_{4141}-\Gamma_{2121}$
$\vec{S}^{(4)}_{13.[1,2]}=-\frac{[\Gamma_{1111},\Gamma_{2222}]\vec{\mu}_{42}\vec{\mu}_{14}\cdot\vec{E}_L\vec{\mu}_{21}\cdot\vec{E}_K\vec{\mu}_{12}\cdot\vec{E}^{\star}_J\vec{\mu}_{21}\cdot\vec{E}_I}{\hbar^4\Gamma_{\text{tot}}}$ $s^{(4)}_{13.[1,2]}=i\omega_{42}-\Gamma_{4242}$	$A^{(4)}_{13.[1,2]}=-i\omega_I+i\omega_{21}+\Gamma_{2121}$ $B^{(4)}_{13.[1,2]}=i\omega_J-i\omega_{21}+[\Gamma_{\text{tot}}-\Gamma_{2121},-\Gamma_{2121}]$ $C^{(4)}_{13.[1,2]}=-i\omega_K+i\omega_{21}+[\Gamma_{2121}-\Gamma_{\text{tot}},\Gamma_{2121}]$ $D^{(4)}_{13.[1,2]}=-i\omega_L-i\omega_{41}+\Gamma_{4242}-\Gamma_{2121}$
$\vec{S}^{(4)}_{14.[1,2]}=-\frac{[\Gamma_{2222},\Gamma_{1111}]\vec{\mu}_{24}\vec{\mu}_{43}\cdot\vec{E}_L\vec{\mu}_{32}\cdot\vec{E}_K\vec{\mu}_{12}\cdot\vec{E}^{\text{☆}}_J\vec{\mu}_{21}\cdot\vec{E}_I}{\hbar^4\Gamma_{\text{tot}}}$ $s^{(4)}_{14.[1,2]}=-i\omega_{42}-\Gamma_{4242}$	$A^{(4)}_{14.[1,2]}=-i\omega_I+i\omega_{21}+\Gamma_{2121}$ $B^{(4)}_{14.[1,2]}=i\omega_J-i\omega_{21}+[\Gamma_{\text{tot}}-\Gamma_{2121},-\Gamma_{2121}]$ $C^{(4)}_{14.[1,2]}=-i\omega_K+i\omega_{32}+[\Gamma_{3232}-\Gamma_{\text{tot}},\Gamma_{3232}]$ $D^{(4)}_{14.[1,2]}=-i\omega_L+i\omega_{43}+\Gamma_{4242}-\Gamma_{3232}$
$\vec{S}^{(4)}_{15.[1,2]}=\frac{[\Gamma_{2222},\Gamma_{1111}]\vec{\mu}_{43}\vec{\mu}_{24}\cdot\vec{E}_L\vec{\mu}_{32}\cdot\vec{E}_K\vec{\mu}_{12}\cdot\vec{E}^{\star}_J\vec{\mu}_{21}\cdot\vec{E}_I}{\hbar^4\Gamma_{\text{tot}}}$ $s^{(4)}_{15.[1,2]}=i\omega_{43}-\Gamma_{4343}$	$A^{(4)}_{15.[1,2]}=-i\omega_I+i\omega_{21}+\Gamma_{2121}$ $B^{(4)}_{15.[1,2]}=i\omega_J-i\omega_{21}+[\Gamma_{\text{tot}}-\Gamma_{2121},-\Gamma_{2121}]$ $C^{(4)}_{15.[1,2]}=-i\omega_K+i\omega_{32}+[\Gamma_{3232}-\Gamma_{\text{tot}},\Gamma_{3232}]$ $D^{(4)}_{15.[1,2]}=-i\omega_L-i\omega_{42}+\Gamma_{4343}-\Gamma_{3232}$
$\vec{S}^{(4)}_{16.[1,2]}=\frac{[\Gamma_{2222},\Gamma_{1111}]\vec{\mu}_{14}\vec{\mu}_{42}\cdot\vec{E}_L\vec{\mu}_{21}\cdot\vec{E}_K\vec{\mu}_{12}\cdot\vec{E}^{\star}_J\vec{\mu}_{21}\cdot\vec{E}_I}{\hbar^4\Gamma_{\text{tot}}}$ $s^{(4)}_{16.[1,2]}=-i\omega_{41}-\Gamma_{4141}$	$A^{(4)}_{16.[1,2]}=-i\omega_I+i\omega_{21}+\Gamma_{2121}$ $B^{(4)}_{16.[1,2]}=i\omega_J-i\omega_{21}+[\Gamma_{\text{tot}}-\Gamma_{2121},-\Gamma_{2121}]$ $C^{(4)}_{16.[1,2]}=-i\omega_K+i\omega_{21}+[\Gamma_{2121}-\Gamma_{\text{tot}},\Gamma_{2121}]$ $D^{(4)}_{16.[1,2]}=-i\omega_L+i\omega_{42}+\Gamma_{4141}-\Gamma_{2121}$

TABLE II. (*Continued*).

$\vec{S}^{(4)}_{17.[1,2]}=-\dfrac{[\Gamma_{2222},\Gamma_{1111}]\vec{\mu}_{42}\vec{\mu}_{14}\cdot\vec{E}_L\vec{\mu}_{21}\cdot\vec{E}_K\vec{\mu}_{12}\cdot\vec{E}^{\star}_J\vec{\mu}_{21}\cdot\vec{E}_I}{\hbar^4\Gamma_{\mathrm{tot}}}$	$A^{(4)}_{17.[1,2]}=-i\omega_I+i\omega_{21}+\Gamma_{2121}$
$s^{(4)}_{17[1,2]}=i\omega_{42}-\Gamma_{4242}$	$B^{(4)}_{17.[1,2]}=i\omega_J-i\omega_{21}+[\Gamma_{\mathrm{tot}}-\Gamma_{2121},-\Gamma_{2121}]$
	$C^{(4)}_{17.[1,2]}=-i\omega_K+i\omega_{21}+[\Gamma_{2121}-\Gamma_{\mathrm{tot}},\Gamma_{2121}]$
	$D^{(4)}_{17.[1,2]}=-i\omega_L-i\omega_{41}+\Gamma_{4242}-\Gamma_{2121}$
$\vec{S}^{(4)}_{18.[1,2]}=\dfrac{[\Gamma_{2222},-\Gamma_{2222}]\vec{\mu}_{14}\vec{\mu}_{42}\cdot\vec{E}_L\vec{\mu}_{21}\cdot\vec{E}_K\vec{\mu}_{12}\cdot\vec{E}^{\star}_J\vec{\mu}_{21}\cdot\vec{E}_I}{\hbar^4\Gamma_{\mathrm{tot}}}$	$A^{(4)}_{18.[1,2]}=-i\omega_I+i\omega_{21}+\Gamma_{2121}$
$s^{(4)}_{18[1,2]}=-i\omega_{41}-\Gamma_{4141}$	$B^{(4)}_{18.[1,2]}=+i\omega_J-i\omega_{21}+[\Gamma_{\mathrm{tot}}-\Gamma_{2121},-\Gamma_{2121}]$
	$C^{(4)}_{18.[1,2]}=-i\omega_K+i\omega_{21}+[\Gamma_{2121}-\Gamma_{\mathrm{tot}},\Gamma_{2121}]$
	$D^{(4)}_{18.[1,2]}=-i\omega_L+i\omega_{42}+\Gamma_{4141}-\Gamma_{2121}$
$\vec{S}^{(4)}_{19.[1,2]}=\dfrac{[-\Gamma_{2222},\Gamma_{2222}]\vec{\mu}_{42}\vec{\mu}_{14}\cdot\vec{E}_L\vec{\mu}_{21}\cdot\vec{E}_K\vec{\mu}_{12}\cdot\vec{E}^{\star}_J\vec{\mu}_{21}\cdot\vec{E}_I}{\hbar^4\Gamma_{\mathrm{tot}}}$	$A^{(4)}_{19.[1,2]}=-i\omega_I+i\omega_{21}+\Gamma_{2121}$
$s^{(4)}_{19.[1,2]}=i\omega_{42}-\Gamma_{4242}$	$B^{(4)}_{19.[1,2]}=i\omega_J-i\omega_{21}+[\Gamma_{\mathrm{tot}}-\Gamma_{2121},-\Gamma_{2121}]$
	$C^{(4)}_{19.[1,2]}=-i\omega_K+i\omega_{21}+[\Gamma_{2121}-\Gamma_{\mathrm{tot}},\Gamma_{2121}]$
	$D^{(4)}_{19.[1,2]}=-i\omega_L-i\omega_{41}+\Gamma_{4242}-\Gamma_{2121}$

where the constants associated to the nineteen pathways are given in Table II. Performing the time integration, the fourth-order polarization in the direction $\vec{k}_{\mathrm{SF}}$ takes the form

$$\begin{aligned}\vec{P}^{(4)}&(I,J,K,L;\vec{k}_{\mathrm{SF}},t)\\&=\sum_{\xi=1}^{35}\overrightarrow{CP}^{(4)}_{\eta}(I,J,K,L;\overline{k}_{\mathrm{SF}},t)\\&=\sum_{\xi=1}^{35}\vec{S}^{(4)}_{\xi}e^{s^{(4)}_{\xi}t}e^{i\vec{k}_{\mathrm{SF}}\cdot\vec{r}}\left[\sum_{\nu=1}^{141}H(t-\lambda^{>}_{\nu\xi})Q^{>}_{\nu\xi}e^{q^{>}_{\nu\xi}t}\right.\\&\quad+\overline{H}(\lambda^{<}_{1\xi}-t)Q^{<}_{1\xi}e^{q^{<}_{1\xi}t}\\&\quad\left.+\sum_{\nu=1}^{220}H(t-\lambda^{\times}_{1,\nu\xi})\overline{H}(\lambda^{\times}_{2,\nu\xi}-t)Q^{\times}_{\nu\xi}e^{q^{\times}_{\nu\xi}t}\right].\end{aligned}\tag{3.15}$$

Notice that ξ runs from 1 to 35 and not to 19, which is the number of different pathways. This is because the pathways involving the evolution of the populations $G_{nnnn}(t_i-t_j)$ or the transfer of the populations $G_{1122}(t_i-t_j)$ give two different contributions. The first one is associated with the exponential term and the second one with the constant term, as we can see from their analytical structure given by relation (3.13). In addition, because of the overlaping between the various light pulses, their interactions with the adsorbed system can take place with different chronological orders. They correspond to the various combinations of the subscripts *I, J, K,* and *L* taken from the three different fields and contributing to the five-wave mixing process. These combinations generate four different types of contributions termed sequential term, self-modulation term, and synchronous and asynchronous interference terms. A detailed analysis of these contributions will be done in the next section.

IV. CONTRIBUTIONS TO THE PUMPED SFG SUSCEPTIBILITY

We first analyze the various terms involved in the pumped sum-frequency generation process. For the sequential term, the pump beam first creates a population which is later tested by the infrared probe and visible probe beams. In relation (3.15), the quantities $\vec{S}^{(4)}_{\xi},\vec{s}^{(4)}_{\xi}$, as well as the various constants Q and q depend on the *I, J, K,* and *L* indices. Therefore, the contribution to the polarization of this sequential term can be expressed as

$$\vec{P}^{(4)}_{\mathrm{sequent}}(\vec{k}_{\mathrm{SF}},t)=\vec{P}^{(4)}(\mathrm{IR,IR,ir,vis};\vec{k}_{\mathrm{SF}},t).\tag{4.1}$$

This is exactly what we get from a usual pump-probe experiment. In the case of the self-modulation term, it is just the probe infrared beam which first populates and next simultaneously with the visible beam probes the system. In this case, we have

$$\vec{P}^{(4)}_{\mathrm{self\text{-}mod.}}(\vec{k}_{\mathrm{SF}},t)=\vec{P}^{(4)}(\mathrm{ir,ir,ir,vis};\vec{k}_{\mathrm{SF}},t).\tag{4.2}$$

Finally, for the interference term, the population is first created by combining the infrared pump and probe beams, and next is tested by the combination of the infrared pump and visible probe beams. We have two different contributions. The synchronous interference term corresponds to two successive interactions with the pump field and generates a contribution given by

$$\vec{P}^{(4)}_{\mathrm{synch.int.}}(\vec{k}_{\mathrm{SF}},t)=\vec{P}^{(4)}(\mathrm{ir,IR,IR,vis};\vec{k}_{\mathrm{SF}},t),\tag{4.3}$$

while for the asynchronous interference term the pump beam interacts alternatively with the infrared probe beam, so that

$$\vec{P}^{(4)}_{\mathrm{asynch.int.}}(\vec{k}_{\mathrm{SF}},t)=\vec{P}^{(4)}(\mathrm{IR,ir,IR,vis};\vec{k}_{\mathrm{SF}},t),\tag{4.4}$$

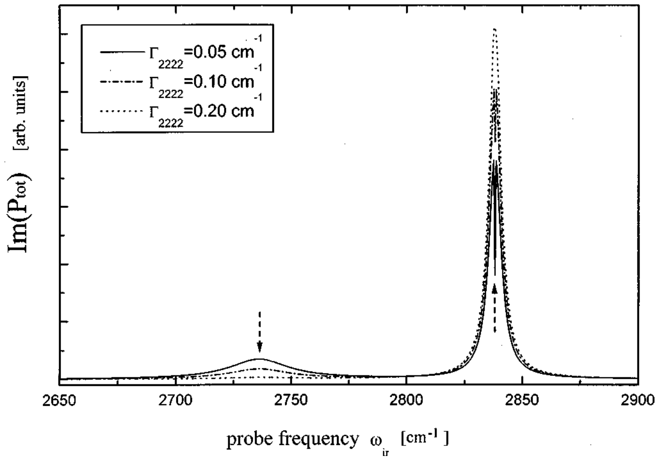

FIG. 2. Calculated spectrum of the total polarization in a pumped sum-frequency experiment. The vibrational dephasing constant Γ_{1212} is equal to 3 cm^{-1}. For our purpose, the field amplitudes are set equal to $\vec{E}(\omega_{\mathrm{IR}})=2\vec{E}(\omega_{\mathrm{ir}})=2\vec{E}(\omega_{\mathrm{vis}})$. The pumping and probing times are chosen equal, $\overline{t_{\mathrm{IR}}}=\overline{t_{\mathrm{ir}}}=\overline{t_{\mathrm{vis}}}=0$, and this is also true for the pumping and probing spectral widths, $\gamma_{\mathrm{IR}}=\gamma_{\mathrm{ir}}=\gamma_{\mathrm{vis}}=10^{-6}\,\mathrm{cm}^{-1}$. In addition, the pumping beam is resonant with the first vibrational transition and $\omega_{\mathrm{vis}}=20\,000\,\mathrm{cm}^{-1}$.

In Fig. 2, we have drawn the imaginary part of the total polarization, $\mathrm{Im}[\vec{P}^{(2)}(\vec{k}_{\mathrm{SF}})+\vec{P}^{(4)}(\vec{k}_{\mathrm{SF}})]$, which gives the frequency dependence of the absorption spectrum

$$\begin{aligned}\mathrm{Im}[\vec{P}^{(2)}(\vec{k}_{\mathrm{SF}})+\vec{P}^{(4)}(\vec{k}_{\mathrm{SF}})] \\ &= \mathrm{Im}[\vec{P}^{(2)}(\mathrm{ir,vis};\vec{k}_{\mathrm{SF}})+\vec{P}^{(4)}_{\mathrm{sequent}}(\vec{k}_{\mathrm{SF}})+\vec{P}^{(4)}_{\text{self-mod.}}(\vec{k}_{\mathrm{SF}}) \\ &\quad +\vec{P}^{(4)}_{\mathrm{synch.int.}}(\vec{k}_{\mathrm{SF}})+\vec{P}^{(4)}_{\mathrm{asynch.int.}}(\vec{k}_{\mathrm{SF}})], \qquad (4.5)\end{aligned}$$

where the trivial time dependence has been omitted. We clearly see the two resonances corresponding to the first and second vibrational transitions in the ground electronic configuration. The dotted arrows show the resonance energy transitions, and the spectra have been drawn for different total decay rates of level 2. For the two lower values of Γ_{2222} the dip is observable, while for higher values it disappears. There are two main reasons for its observability. The first one is quite trivial and results from the fact that the dip comes from the interference term of $\vec{P}^{(4)}(\vec{k}_{\mathrm{SF}},t)$ alone. Since the five-wave-mixing polarization mixes contributions of the second and fourth order, if the condition $|\vec{P}^{(2)}(\vec{k}_{\mathrm{SF}},t)| \gg |\vec{P}^{(4)}(\vec{k}_{\mathrm{SF}},t)|$ is satisfied, the dip will be washed out. This situation can be avoided by a convenient choice of the field amplitudes and polarizations. The other one arises from the internal dynamics of the adsorbed system driven by the relaxation and dephasing constants. This is the point which is emphasized in this figure, showing the total absorption spectrum. We observe the disappearance of the dip for increasing values of the vibrational total decay rate Γ_{2222}. To go further, we will analyze the influence of the pure vibrational dephasing processes on the frequency spectra of the various sequential, self-modulation, synchronous, and asynchronous interference terms, previously defined. The different terms are represented with the same arbitrary scale in Fig. 3, and

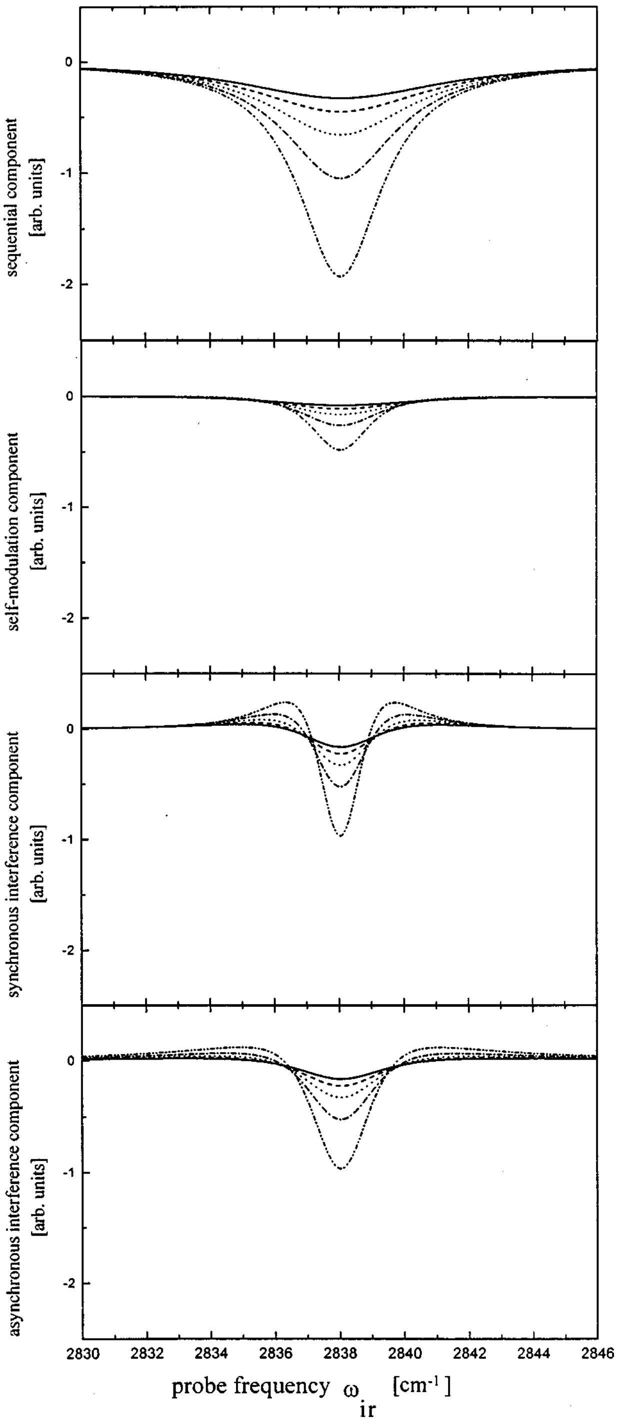

FIG. 3. Influence of the pure vibrational dephasing processes on the polarization corresponding to the five-wave-mixing process alone. The various contributions to the imaginary part of $\vec{P}^{(4)}(\vec{k}_{\mathrm{SF}},t)$ are analyzed separately. The cases $\Gamma^{(d)}_{12}$ equal to 2.8 cm^{-1} (——), 2.2 cm^{-1} (- - -), 1.7 cm^{-1} (·····), 1.1 cm^{-1} (- · - ·), and 0.6 cm^{-1} (- · · · -) are considered. The total decay rate is set equal to $\Gamma_{2222}=2$ cm^{-1}. Other values are identical to those used in Fig. 2.

are of comparable magnitude. Therefore, really both synchronous and asynchronous interference terms must be accounted for to analyze the dip. While the sequential and self-modulation terms show a characteristic dip structure resulting in a decrease of the absorption at the center of the

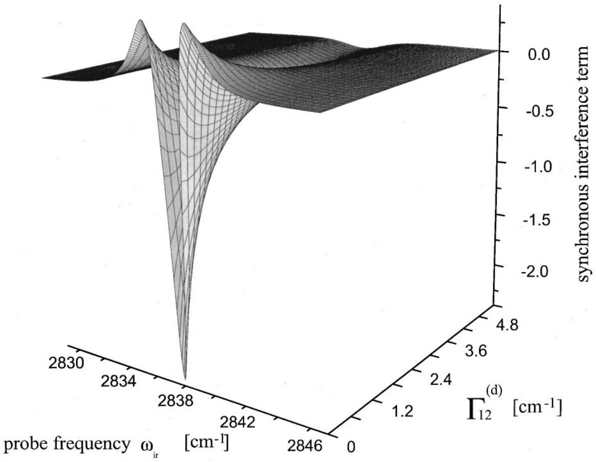

FIG. 4. Representation of the synchronous interference term as a function of the probe frequency and pure vibrational dephasing for the five-wave-mixing process alone. The various constants are the ones used in Fig. 3.

line shape, both interference terms show, symmetrically around the dip zone, an enhancement of the absorption. With respect to the influence of the pure vibrational dephasing, all the terms are similarly influenced and show a continuous decrease of the dip structure for increasing pure vibrational dephasing. Notice that the asynchronous term is spectrally wider and has a smaller absorption enhancement than the synchronous one. To stress the importance of the asynchronous term with respect to the synchronous one, we map the variations of the synchronous interference term $\vec{P}^{(4)}_{\text{synch.int.}}(\vec{k}_{\text{SF}},t)$ in Fig. 4 as a function of both the infrared probe frequency and the pure vibrational dephasing. Similar variations are shown in Fig. 5, for the asynchronous term $\vec{P}^{(4)}_{\text{asynch.int.}}(\vec{k}_{\text{SF}},t)$. We note that both interference terms have similar behavior, even if the asynchronous contribution is spectrally wider. However, the decrease of the dip is comparable for both terms. This demonstrates the high sensitivity of the dip to the pure dephasing processes.

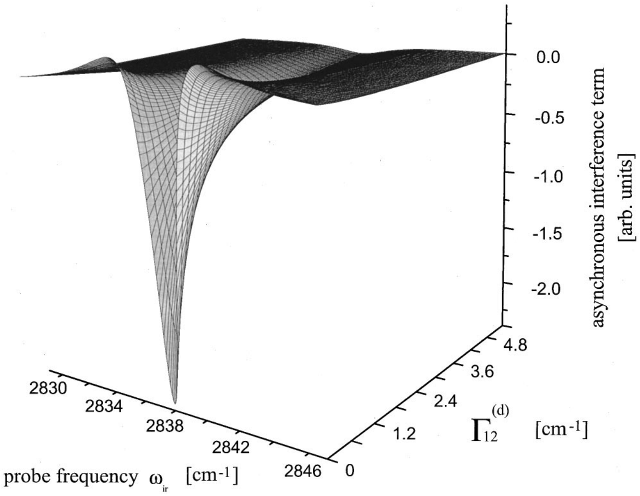

FIG. 5. Variations of the asynchronous interference term obtained for the same parameters previously used in Fig. 4 for the synchronous term.

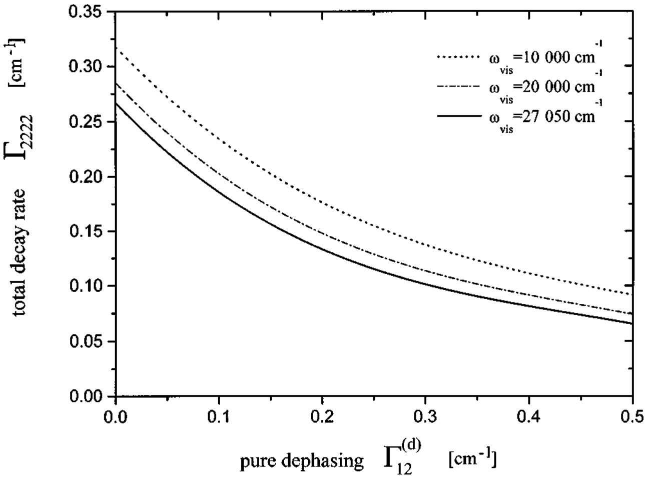

FIG. 6. We draw the set of conjugated values $(\Gamma_{2222},\Gamma_{12}^{(d)})$ which cancels the second derivative of the total absorption spectrum $\mathrm{Im}[\vec{P}^{(2)}(\vec{k}_{\mathrm{SF}},t)+\vec{P}^{(4)}(\vec{k}_{\mathrm{SF}},t)]$. The region enclosed between the vertical axis Γ_{2222}, the horizontal axis $\Gamma_{12}^{(d)}$, and the curve is the zone where the dip exists. The cases of different probe visible frequencies are considered. Other values are identical to the ones used in Fig. 3.

V. OBSERVABILITY OF THE DIP IN PUMPED SUM-FREQUENCY GENERATION EXPERIMENT

The experimental determination of the dip can only be done through the measurement of the pumped sum-frequency signal involving the second-order background and the five-wave-mixing contribution. This implies, in turn, that the conditions for its observability come through the total polarization $[\vec{P}^{(2)}(\vec{k}_{\mathrm{SF}})+\vec{P}^{(4)}(\vec{k}_{\mathrm{SF}})]$. A quite simple way to define the region where the dip exists is obtained from the

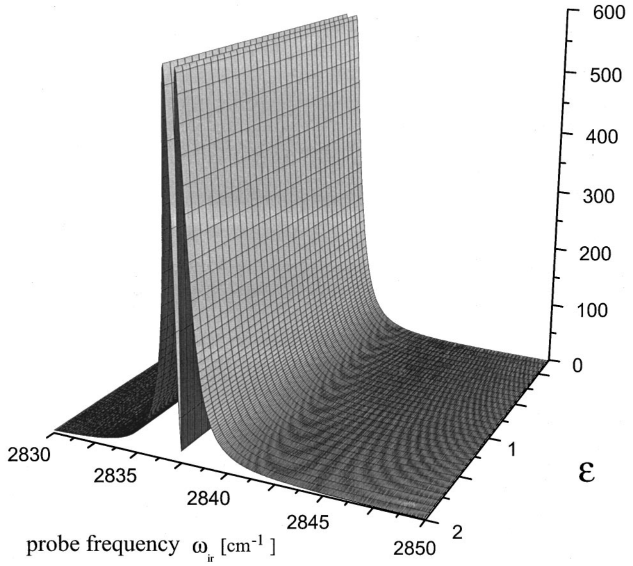

FIG. 7. Total absorption spectra as a function of the infrared probe frequency and the pure electronic dephasing defined as $\Gamma_{i4}^{(d)}=\epsilon\times 30\,\mathrm{cm}^{-1}$ for $i=1$ to 3. The visible probe frequency is set nonresonant with the electronic transition and corresponds to $\omega_{\mathrm{vis}}=20\,000\,\mathrm{cm}^{-1}$. All the other values are identical to those used in Fig. 3.

curvature of the total absorption profile which corresponds to the imaginary part of the total polarization. When the second-order derivative of the total absorption profile with respect to the infrared probe frequency is positive, a dip exists on the frequency spectrum. To define the set of pairs $(\Gamma^{12}_{(d)},\Gamma_{2222})$ ensuring the existence of the dip, we have drawn, in Fig. 6, the curve corresponding to the zero value of the second derivative given by

$$\begin{aligned}
0=\mathrm{Im}\Bigg\{ & \sum_{\eta=1}^{2} \vec{S}^{(2)}_{\eta} e^{s^{(2)}_{\eta}t}\Bigg[\sum_{\beta=1}^{7} H(t-\tau^{>}_{\beta\eta})\left(\frac{d^2D^{>}_{\beta\eta}}{d\omega^2_{\mathrm{ir}}}+2\,\frac{dD^{>}_{\beta\eta}}{d\omega_{\mathrm{ir}}}\,\frac{dd^{>}_{\beta\eta}}{d\omega_{\mathrm{ir}}}+D^{>}_{\beta\eta}\frac{d^2d^{>}_{\beta\eta}}{d\omega^2_{\mathrm{ir}}}+D^{>}_{\beta\eta}\left[\frac{dd^{>}_{\beta\eta}}{d\omega_{\mathrm{ir}}}\right]^2\right)e^{d^{>}_{\beta\eta}t} \\
& +\overline{H}(\tau^{<}_{1\eta}-t)\left(\frac{d^2D^{<}_{1\eta}}{d\omega^2_{\mathrm{ir}}}+2\,\frac{dD^{<}_{1\eta}}{d\omega_{\mathrm{ir}}}\,\frac{dd^{<}_{1\eta}}{d\omega_{\mathrm{ir}}}+D^{<}_{1\eta}\frac{d^2d^{<}_{1\eta}}{d\omega^2_{\mathrm{ir}}}+D^{<}_{1\eta}\left[\frac{dd^{<}_{1\eta}}{d\omega_{\mathrm{ir}}}\right]^2\right)e^{d^{<}_{1\eta}t} \\
& +\sum_{\beta=1}^{6} H(t-\tau^{\times}_{1,\beta\eta})\overline{H}(\tau^{\times}_{2,\beta\eta}-t)\left(\frac{d^2D^{\times}_{\beta\eta}}{d\omega^2_{\mathrm{ir}}}+2\,\frac{dD^{\times}_{\beta\eta}}{d\omega_{\mathrm{ir}}}\,\frac{dd^{\times}_{\beta\eta}}{d\omega_{\mathrm{ir}}}+D^{\times}_{\beta\eta}\frac{d^2d^{\times}_{\beta\eta}}{d\omega^2_{\mathrm{ir}}}+D^{\times}_{\beta\eta}\left[\frac{dd^{\times}_{\beta\eta}}{d\omega_{\mathrm{ir}}}\right]^2\right)e^{d^{\times}_{\beta\eta}t}\Bigg] \\
& +\sum_{\xi=1}^{35} \vec{S}^{(4)}_{\xi} e^{s^{(4)}_{\xi}t}\Bigg[\sum_{\nu=1}^{141} H(t-\lambda^{>}_{\nu\xi})\left(\frac{d^2Q^{>}_{\nu\eta}}{d\omega^2_{\mathrm{ir}}}+2\,\frac{dQ^{>}_{\nu\eta}}{d\omega_{\mathrm{ir}}}\,\frac{dq^{>}_{\nu\eta}}{d\omega_{\mathrm{ir}}}+Q^{>}_{\nu\eta}\frac{d^2q^{>}_{\nu\eta}}{d\omega^2_{\mathrm{ir}}}+Q^{>}_{\nu\eta}\left[\frac{dq^{>}_{\nu\eta}}{d\omega_{\mathrm{ir}}}\right]^2\right)e^{q^{>}_{\nu\xi}t} \\
& +\overline{H}(\lambda^{<}_{1\xi}-t)\left(\frac{d^2Q^{<}_{1\eta}}{d\omega^2_{\mathrm{ir}}}+2\,\frac{dQ^{<}_{1\eta}}{d\omega_{\mathrm{ir}}}\,\frac{dq^{<}_{1\eta}}{d\omega_{\mathrm{ir}}}+Q^{<}_{1\eta}\frac{d^2q^{<}_{1\eta}}{d\omega^2_{\mathrm{ir}}}+Q^{<}_{1\eta}\left[\frac{dq^{<}_{1\eta}}{d\omega_{\mathrm{ir}}}\right]^2\right)e^{q^{<}_{1\xi}t} \\
& +\sum_{\nu=1}^{220} H(t-\lambda^{\times}_{1,\nu\xi})\overline{H}(\lambda^{\times}_{2,\nu\xi}-t)\left(\frac{d^2Q^{\times}_{\nu\eta}}{d\omega^2_{\mathrm{ir}}}+2\,\frac{dQ^{\times}_{\nu\eta}}{d\omega_{\mathrm{ir}}}\,\frac{dq^{\times}_{\nu\eta}}{d\omega_{\mathrm{ir}}}+Q^{\times}_{\nu\eta}\frac{d^2q^{\times}_{\nu\eta}}{d\omega^2_{\mathrm{ir}}}+Q^{\times}_{\nu\eta}\left[\frac{dq^{\times}_{\nu\eta}}{d\omega_{\mathrm{ir}}}\right]^2\right)e^{q^{\times}_{\nu\xi}t}\Bigg]\Bigg\}. \qquad (5.1)
\end{aligned}$$

Three different visible probe frequencies have been considered. For each visible probe frequency, the region where a dip is observable is enclosed by the curve defined in relation (5.1), the horizontal axis $\Gamma^{12}_{(d)}$ and the vertical axis Γ_{2222}. From this simulation, we note that the region where the dip is observable increases as much as the visible field frequency gets away from the electronic transition frequency.

Up to now, we have been concerned with the influence of the pure vibrational dephasing. However, when populations are tested by the conjugated infrared and visible probe beams, the electronic transition contributes to the dynamics. It is interesting to analyze the influence of the pure electronic dephasing taking place between the excited electronic configuration described by the level 4 and the various vibrational states of the ground electronic configuration. To this end, we parametrize the pure electronic constants by the parameter ϵ like

$$\Gamma_{i4i4}=\tfrac{1}{2}[\Gamma_{iiii}+\Gamma_{4444}]+\epsilon\Gamma^{(d)}_{\mathrm{el}}, \quad i=1-3$$

since all the pure electronic dephasing constants associated to the various ground vibrational levels must be influenced similarly. First, we consider the case of a nonresonant visible probe beam. In Fig. 7, we draw the variations of the total absorption spectrum as a function of the infrared probe frequency for different pure electronic dephasings. It clearly appears, as can be expected in such a nonresonant situation, that pure electronic dephasing does not influence the aborption spectrum leaving the dip structure unchanged. This is not true anymore when the visible probe field is such that the SFG signal becomes near-resonant with the electronic transition. We have reported in Fig. 8 the same variations as in Fig. 7, except that the visible probe frequency is now comparable to the electronic transition frequency. Here, we see that for small values of the pure electronic dephasings, the dip structure obtained in the nonresonant case is recovered. However, for increasing values of the pure electronic dephasing, the dip becomes asymmetric with a decrease of the peak stronger on the blue frequency side than on the red frequency side, as it can be seen from the inset. In addition, we note that the pure electronic dephasing increases the absorption on the red side while it decreases on the blue side, where even induced emission can be obtained, as is the case for the value $\epsilon=2$. Finally, we represent in Fig. 9 the variations of the total absorption spectrum as a function of both the infrared probe frequency and the pure vibrational dephasing. We observe a strong attenuation of the dip structure induced by the vibrational dephasing processes. Yet, for pure vibrational dephasing constants of the order of the vibrational total decay rate, the dip has been severely washed out. However, contrary to what is observed for pure electronic dephasing, here the symmetry of the dip structure is preserved.

VI. CONCLUSION

In the present work, we have developed a unified description of five-wave mixing which is valid for the full scale of the dephasing times. The same methodology can be applied to the study of any type of wave mixing provided that the spectral decomposition of the Liouvillian evolution operator can be obtained. This is due to the fact that the multiple time integral involving this type of pulse shape results in a recurrent form which can be extended to higher order. This theory has been applied, here, to the particular case of pumped sum-frequency generation spectroscopy, which appears to be very powerful to study and test bonding processes on adsorption,

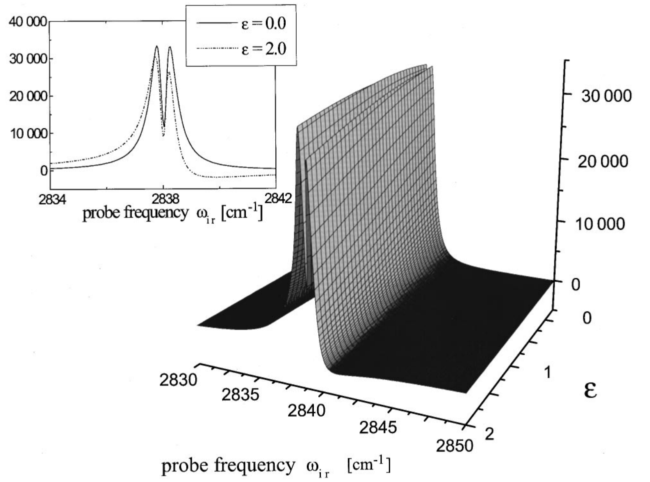

FIG. 8. We show, for a visible probe field near-resonant with the electronic transition, the same variations previously given in Fig. 7. The visible probe field frequency corresponds to $\omega_{\text{vis}}=27\,050\ \text{cm}^{-1}$. All the other values are set as in Fig. 7.

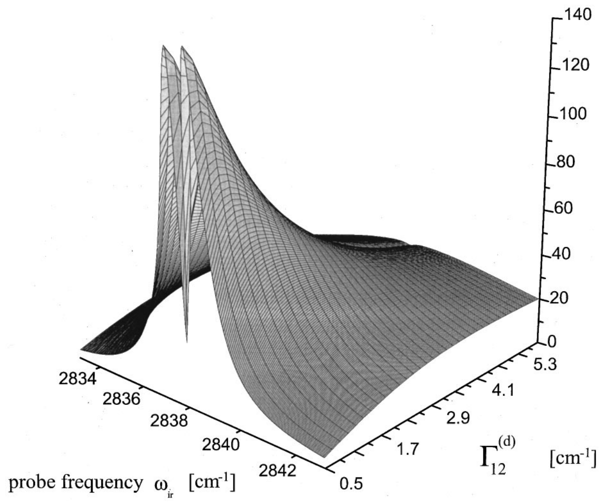

FIG. 9. Total absorption spectra in the vicinity of the dip structure. The attenuation of the dip induced by the pure vibrational dephasing is emphasized. All the physical constants are set identical to the ones of Fig. 3.

as well as molecule-surface reactions [27,28]. We have clearly established the origin of the contributions to the dip located at the center of the vibrational absorption spectrum. In particular, the contribution of a new additional asynchronous interference term has been demonstrated and is comparable in magnitude to the synchronous interference term previously discussed. The influence of the pure vibrational or electronic dephasing on the dip has been analyzed. The pure vibrational dephasing plays a dominant role and can wash out the dip for dephasing time comparable to the excited lifetimes. In addition, this approach opens new possibilities to study the influence of the vibrational and electronic dephasings on the time dependence of the transient sum-frequency signals, which were previously limited to very short dephasing times. Also, more complex situations involving time-delayed probe pulses [29,30], which are required for the study of the dephasing processes in the hot vibrational bands, can now be handled. This problem is currently under investigation.

APPENDIX A

In this appendix, we introduce the formal expression of the double time integral required in the text. It takes the form

$$\mathcal{I}_{\eta}^{(2)}(t)=\int_{-\infty}^{t} dt_2 e^{B_{\eta}t_2}e^{-\gamma_j|t_2-\overline{t_j}|}\int_{-\infty}^{t_2} dt_1 e^{A_{\eta}t_1}e^{-\gamma_i|t_1-\overline{t_i}|}$$
$$=\sum_{\nu=1}^{7} H(t-\tau_{\nu\eta}^{>})D_{\nu\eta}^{>}e^{d_{\nu\eta}^{>}t}+\overline{H}(\tau_{1\eta}^{<}-t)D_{1\eta}^{<}e^{d_{1\eta}^{<}t}+\sum_{\nu=1}^{6} H(t-\tau_{1,\nu\eta}^{\times})\overline{H}(\tau_{2,\nu\eta}^{\times}-t)D_{\nu\eta}^{\times}e^{d_{\nu\eta}^{\times}t}. \tag{A1}$$

The various constants resulting from the first time integration over t_1 are given by

$$P_{1\eta}^{>}=\frac{e^{A_{\eta}\overline{t_i}}}{A_{\eta}+\gamma_i}-\frac{e^{A_{\eta}\overline{t_i}}}{A_{\eta}-\gamma_i},\quad p_{1\eta}^{>}=0,\quad P_{2\eta}^{>}=\frac{e^{\gamma_i\overline{t_i}}}{A_{\eta}-\gamma_i},\quad p_{2\eta}^{>}=A_{\eta}-\gamma_i,\quad P_{1\eta}^{<}=\frac{e^{-\gamma_i\overline{t_i}}}{A_{\eta}+\gamma_i},\quad p_{1\eta}^{<}=A_{\eta}+\gamma_i, \tag{A2}$$

and the second time integration over t_2 generates the constants

$$\begin{aligned}
&D_{1\eta}^{>}=P_{1\eta}^{<}e^{-\gamma_j\overline{t_j}}I(T_{ij}^{<},B_{\eta}+p_{1\eta}^{<}+\gamma_j), && d_{1\eta}^{>}=0, && \tau_{1\eta}^{>}=T_{ij}^{<},\\
&D_{2\eta}^{>}=H(\overline{t_j}-\overline{t_i})\sum_{\alpha=1}^{2} P_{\alpha\eta}^{>}e^{-\gamma_j\overline{t_j}}J(\overline{t_j},\overline{t_i},B_{\eta}+p_{\alpha\eta}^{>}+\gamma_j), && d_{2\eta}^{>}=0, && \tau_{2\eta}^{>}=\overline{t_j},\\
&D_{3\eta}^{>}=\overline{H}(\overline{t_i}-\overline{t_j})P_{1\eta}^{<}e^{\gamma_j\overline{t_j}}J(\overline{t_i},\overline{t_j},B_{\eta}+p_{1\eta}^{<}-\gamma_j), && d_{3\eta}^{>}=0, && \tau_{3\eta}^{>}=\overline{t_i},\\
&D_{4\eta}^{>}=P_{1\eta}^{>}e^{\gamma_j\overline{t_j}}(B_{\eta}+p_{1\eta}^{>}-\gamma_j)^{-1}, && d_{4\eta}^{>}=B_{\eta}+p_{1\eta}^{>}-\gamma_j, && \tau_{4\eta}^{>}=T_{ij}^{>},\\
&D_{5\eta}^{>}=P_{2\eta}^{>}e^{\gamma_j\overline{t_j}}(B_{\eta}+p_{2\eta}^{>}-\gamma_j)^{-1}, && d_{5\eta}^{>}=B_{\eta}+p_{2\eta}^{>}-\gamma_j, && \tau_{5\eta}^{>}=T_{ij}^{>},
\end{aligned} \tag{A3}$$

$$
\begin{aligned}
&D^{>}_{6\eta}=-P^{>}_{1\eta}e^{\gamma_j\overline{t_j}}I(T^{>}_{ij},B_\eta+p^{>}_{1\eta}-\gamma_j), && d^{>}_{6\eta}=0, && \tau^{>}_{6\eta}=T^{>}_{ij},\\
&D^{>}_{7\eta}=-P^{>}_{2\eta}e^{\gamma_j\overline{t_j}}I(T^{>}_{ij},B_\eta+p^{>}_{2\eta}-\gamma_j), && d^{>}_{7\eta}=0, && \tau^{>}_{7\eta}=T^{>}_{ij},\\
&D^{<}_{1\eta}=P^{<}_{1\eta}e^{-\gamma_j\overline{t_j}}(B_\eta+p^{<}_{1\underline{\eta}}+\gamma_j)^{-1}, && d^{<}_{1\eta}=B_\eta+p^{<}_{1\eta}+\gamma_j, && \tau^{<}_{1\eta}=T^{<}_{ij},\\
&D^{\times}_{1\eta}=H(\overline{t_j}-\overline{t_i})P^{>}_{1\eta}e^{-\gamma_j\overline{t_j}}(B_\eta+p^{>}_{1\eta}+\gamma_j)^{-1}, && d^{\times}_{1\eta}=B_\eta+p^{>}_{1\eta}+\gamma_j, && \tau^{\times}_{1,1\eta}=\overline{t_i},\\
& && && \tau^{\times}_{2,1\eta}=\overline{t_j},\\
&D^{\times}_{2\eta}=H(\overline{t_j}-\overline{t_i})P^{>}_{2\eta}e^{-\gamma_j\overline{t_j}}(B_\eta+p^{>}_{2\eta}+\gamma_j)^{-1}, && d^{\times}_{2\eta}=B_\eta+p^{>}_{2\eta}+\gamma_j, && \tau^{\times}_{1,2\eta}=\overline{t_i},\\
& && && \tau^{\times}_{2,2\eta}=\overline{t_j},\\
&D^{\times}_{3\eta}=-H(\overline{t_j}-\overline{t_i})P^{>}_{1\eta}e^{-\gamma_j\overline{t_j}}I(\overline{t_i},B_\eta+p^{>}_{1\eta}+\gamma_j), && d^{\times}_{3\eta}=0, && \tau^{\times}_{1,3\eta}=\overline{t_i},\\
& && && \tau^{\times}_{2,3\eta}=\overline{t_j},\\
&D^{\times}_{4\eta}=-H(\overline{t_j}-\overline{t_i})P^{>}_{2\eta}e^{-\gamma_j\overline{t_j}}I(\overline{t_i},B_\eta+p^{>}_{2\eta}+\gamma_j), && d^{\times}_{4\eta}=0, && \tau^{\times}_{1,4\eta}=\overline{t_i},\\
& && && \tau^{\times}_{2,4\eta}=\overline{t_j},\\
&D^{\times}_{5\eta}=\overline{H}(\overline{t_i}-\overline{t_j})P^{<}_{1\eta}e^{\gamma_j\overline{t_j}}(B_\eta+p^{<}_{1\eta}-\gamma_j)^{-1}, && d^{\times}_{5\eta}=B_\eta+p^{<}_{1\eta}-\gamma_j, && \tau^{\times}_{1,5\eta}=\overline{t_j},\\
& && && \tau^{\times}_{2,5\eta}=\overline{t_i},\\
&D^{\times}_{6\eta}=-\overline{H}(\overline{t_i}-\overline{t_j})P^{<}_{1\eta}e^{\gamma_j\overline{t_j}}I(\overline{t_j},B_\eta+p^{<}_{1\eta}-\gamma_j), && d^{\times}_{6\eta}=0, && \tau^{\times}_{1,6\eta}=\overline{t_j},\\
& && && \tau^{\times}_{2,6\eta}=\overline{t_i},
\end{aligned}
$$

with the additional notations

$$
\begin{aligned}
&T^{>}_{ij}=\sup(\overline{t_i},\overline{t_j}),\quad T^{<}_{ij}=\inf(\overline{t_i},\overline{t_j}),\\
&I(t,A)\equiv e^{At}/A,\quad J(t_1,t_2,A)\equiv(e^{At_1}-e^{At_2})/A.
\end{aligned}
\tag{A4}
$$

where “sup” and “inf” stand for the greater and the smaller term, respectively. Notice that all the constants generated by the second time integration depend on the constants arising from the first time integration.

APPENDIX B

Taking advantage of the expressions given in Appendix A, the time integration over t_3 is given by the formal expression

$$
\begin{aligned}
\mathcal{I}^{(3)}_{\eta}(t)&=\int_{-\infty}^{t}dt_3e^{C_\eta t_3}e^{-\gamma_k|t_3-\overline{t_k}|}\mathcal{I}^{(2)}_{\eta}(t_3)\\
&=\sum_{\delta=1}^{29}H(t-\theta^{>}_{\delta\eta})F^{>}_{\delta\eta}e^{f^{>}_{\delta\eta}t}+\overline{H}(\theta^{<}_{1\eta}-t)F^{<}_{1\eta}e^{f^{<}_{1\eta}t}\\
&\quad+\sum_{\delta=1}^{40}H(t-\theta^{\times}_{1,\delta\eta})\overline{H}(\theta^{\times}_{2,\delta\eta}-t)F^{\times}_{\delta\eta}e^{f^{\times}_{\delta\eta}t},
\end{aligned}
\tag{B1}
$$

where the various constants correspond to

$$
\begin{aligned}
&T^{<}_{k;1\eta<}=\inf(\overline{t_k},\tau^{<}_{1\eta}),\quad T^{>}_{k;\beta\eta>}=\sup(\overline{t_k},\tau^{>}_{\beta\eta}),\\
&T^{>}_{k;i\beta\eta\times}=\sup(\overline{t_k},\tau^{\times}_{i\beta\eta}),\quad T^{<}_{k;i\beta\eta\times}=\inf(\overline{t_k},\tau^{\times}_{i\beta\eta}),
\end{aligned}
\tag{B2}
$$

and

$$
\begin{aligned}
&F^{>}_{\delta=1\rightarrow7,\eta}=D^{>}_{\delta\eta}e^{\gamma_k\overline{t_k}}(C_\eta+d^{>}_{\delta\eta}-\gamma_k)^{-1}, && f^{>}_{\delta\eta}=C_\eta+d^{>}_{\delta\eta}-\gamma_k,\\
& && \theta^{>}_{\delta\eta}=T^{>}_{k,\delta\eta>},\\
&F^{>}_{\delta=8\rightarrow14,\eta}=-D^{>}_{(\delta-7)\eta}e^{\gamma_k\overline{t_k}}I(T^{>}_{k,(\delta-7)\eta>},C_\eta+\delta^{>}_{(\delta-7)\eta}-\gamma_k), && f^{>}_{\delta\eta}=0,\\
& && \theta^{>}_{\delta\eta}=T^{>}_{k,(\delta-7)\eta>},\\
&F^{>}_{\delta=15,\eta}=D^{<}_{1\eta}e^{\gamma_k\overline{t_k}}H(\tau^{<}_{1\eta}-\overline{t_k})J(\tau^{<}_{1\eta},\overline{t_k},C_\eta+d^{<}_{1\eta}-\gamma_k), && f^{>}_{\delta\eta}=0,\\
& && \theta^{>}_{\delta\eta}=\tau^{<}_{1\eta},\\
&F^{>}_{\delta=16,\eta}=\sum_{\beta=1}^{141}D^{>}_{\beta\eta}e^{-\gamma_k\overline{t_k}}\overline{H}(\overline{t_k}-\tau^{>}_{\beta\eta})J(\overline{t_k},\tau^{>}_{\beta\eta},C_\eta+d^{>}_{\beta\eta}+\gamma_k), && f^{>}_{\delta\eta}=0,\\
& && \theta^{>}_{\delta\eta}=\overline{t_k},\\
&F^{>}_{\delta=17,\eta}=D^{<}_{1\eta}e^{-\gamma_k\overline{t_k}}I(T^{<}_{k;1\eta<},C_\eta+d^{<}_{1\eta}+\gamma_k), && f^{>}_{\delta\eta}=0,\\
& && \theta^{>}_{\delta\eta}=T^{<}_{k;1\eta<},
\end{aligned}
\tag{B3}
$$

$$\begin{aligned}
F^{>}_{\delta=18\to23,\eta}&=D^{\times}_{(\delta-17)\eta}e^{\gamma_k\bar{t}_k}H(\tau^{\times}_{2,(\delta-17)\eta}-T^{>}_{k;1,(\delta-17)\eta\times}) && f^{>}_{\delta\eta}=0,\\
&\quad\times J(\tau^{\times}_{2,(\delta-17)\eta},T^{>}_{k;1,(\delta-17)\eta\times},C_\eta+d^{\times}_{(\delta-17)\eta}-\gamma_k), && \theta^{>}_{\delta\eta}=\tau^{\times}_{2,(\delta-17)\eta},\\
F^{>}_{\delta=24\to29,\eta}&=D^{\times}_{(\delta-23)\eta}e^{-\gamma_k\bar{t}_k}\bar{H}(T^{<}_{k;2,(\delta-23)\eta\times}-\tau^{\times}_{1,(\delta-23)\eta}) && f^{>}_{\delta\eta}=0,\\
&\quad\times J(T^{<}_{k;2,(\delta-23)\eta\times},\tau^{\times}_{1,(\delta-23)\eta},C_\eta+d^{\times}_{(\delta-23)\eta}+\gamma_k), && \theta^{>}_{\delta\eta}=T^{<}_{k;2,(\delta-23)\eta\times},\\
F^{<}_{\delta=1,\eta}&=D^{<}_{\delta\eta}e^{-\gamma_k t_k}(C_\eta+d^{<}_{\delta\eta}+\gamma_k)^{-1} && f^{<}_{\delta\eta}=C_\eta+d^{<}_{\delta\eta}+\gamma_k,\\
& && \theta^{<}_{\delta\eta}=T^{<}_{k;\delta\eta<},\\
F^{\times}_{\delta=1,\eta}&=D^{<}_{\delta\eta}e^{\gamma_k\bar{t}_k}H(\tau^{<}_{\delta\eta}-\bar{t}_k)(C_\eta+d^{<}_{\delta\eta}-\gamma_k)^{-1}, && f^{\times}_{\delta\eta}=C_\eta+d^{<}_{\delta\eta}-\gamma_k,\\
& && \theta^{\times}_{1,\delta\eta}=\bar{t}_k,\\
& && \theta^{\times}_{2,\delta\eta}=\tau^{<}_{\delta\eta},\\
F^{\times}_{\delta=2,\eta}&=-D^{<}_{(\delta-1)\eta}e^{\gamma_k\bar{t}_k}H(\tau^{<}_{(\delta-1)\eta}-\bar{t}_k)I(\bar{t}_k,C_\eta+d^{<}_{(\delta-1)\eta}-\gamma_k), && f^{\times}_{\delta\eta}=0,\\
& && \theta^{\times}_{1,\delta\eta}=\bar{t}_k,\\
& && \theta^{\times}_{2,\delta\eta}=\tau^{<}_{(\delta-1)\eta},\\
F^{\times}_{\delta=3\to9,\eta}&=D^{>}_{(\delta-2)\eta}e^{-\gamma_k\bar{t}_k}\bar{H}(\bar{t}_k-\tau^{>}_{(\delta-2)\eta})(C_\eta+\delta^{>}_{(\delta-2)\eta}+\gamma_k)^{-1}, && f^{\times}_{\delta\eta}=C_\eta+d^{>}_{(\delta-2)\eta}+\gamma_k,\\
& && \theta^{\times}_{1,\delta\eta}=\tau^{>}_{(\delta-2)\eta},\\
& && \theta^{\times}_{2,\delta\eta}=\bar{t}_k,\\
F^{\times}_{\delta=10\to16,\eta}&=-D^{>}_{(\delta-9)\eta}e^{-\gamma_k\bar{t}_k}\bar{H}(\bar{t}_k-\tau^{>}_{(\delta-9)\eta}) && f^{\times}_{\delta\eta}=0,\\
&\quad\times I(\tau^{>}_{(\delta-9)\eta},C_\eta+d^{>}_{(\delta-9)\eta}+\gamma_k), && \theta^{\times}_{1,\delta\eta}=\tau^{>}_{(\delta-9)\eta},\\
& && \theta^{\times}_{2,\delta\eta}=\bar{t}_k,\\
F^{\times}_{\delta=17\to22,\eta}&=D^{\times}_{(\delta-16)\eta}e^{\gamma_k\bar{t}_k}H(\tau^{\times}_{2,(\delta-16)\eta}-T^{>}_{k;1,(\delta-16)\eta\times}) && f^{\times}_{\delta\eta}=C_\eta+d^{\times}_{(\delta-16)\eta}-\gamma_k,\\
&\quad\times(C_\eta+d^{\times}_{(\delta-16)\eta}-\gamma_k)^{-1}, && \theta^{\times}_{1,\delta\eta}=T^{>}_{k;1,(\delta-16)\eta\times},\\
& && \theta^{\times}_{2,\delta\eta}=\tau^{\times}_{2,(\delta-16)\eta},\\
F^{\times}_{\delta=23\to28,\eta}&=-D^{\times}_{(\delta-22)\eta}e^{\gamma_k\bar{t}_k}H(\tau^{\times}_{2,(\delta-22)\eta}-T^{>}_{k;1,(\delta-22)\eta\times}) && f^{\times}_{\delta\eta}=0,\\
&\quad\times I(T^{>}_{k;1,(\delta-22)\eta\times},C_\eta+d^{\times}_{(\delta-22)\eta}-\gamma_k), && \theta^{\times}_{1,\delta\eta}=T^{>}_{k;1,(\delta-22)\eta\times},\\
& && \theta^{\times}_{2,\delta\eta}=\tau^{\times}_{2,(\delta-22)\eta},\\
F^{\times}_{\delta=29\to34,\eta}&=D^{\times}_{(\delta-28)\eta}e^{-\gamma_k\bar{t}_k}H(T^{<}_{k;2,(\delta-28)\eta\times}-\tau^{\times}_{1,(\delta-28)\eta}) && f^{\times}_{\delta\eta}=C_\eta+d^{\times}_{(\delta-28)\eta}+\gamma_k,\\
&\quad\times(C_\eta+d^{\times}_{(\delta-28)\eta}+\gamma_k)^{-1}, && \theta^{\times}_{1,\delta\eta}=\tau^{\times}_{1,(\delta-28)\eta},\\
& && \theta^{\times}_{2,\delta\eta}=T^{<}_{k;2,(\delta-28)\eta\times},\\
F^{\times}_{\delta=35\to40,\eta}&=-D^{\times}_{(\delta-34)\eta}e^{-\gamma_k\bar{t}_k}H(T^{<}_{k;2,(\delta-34)\eta\times}-\tau^{\times}_{1,(\delta-34)\eta}) && f^{\times}_{\delta\eta}=0,\\
&\quad\times I(\tau^{\times}_{1,(\delta-34)\eta},C_\eta+d^{\times}_{(\delta-34)\eta}+\gamma_k), && \theta^{\times}_{1,\delta\eta}=\tau^{\times}_{1,(\delta-34)\eta},\\
& && \theta^{\times}_{2,\delta\eta}=T^{<}_{k;2,(\delta-34)\eta\times}.
\end{aligned}$$

Finally, the last time integration over t_4, appearing in the text, is given by

$$\begin{aligned}
\mathcal{I}^{(4)}_{\eta}(t)&=\int_{-\infty}^{t}dt_4e^{D_\eta t_4}e^{-\gamma_l|t_4-\bar{t}_1|}\mathcal{I}^{(3)}_{\eta}(t_4)\\
&=\sum_{\nu=1}^{141}H(t-\lambda^{>}_{\nu\eta})Q^{>}_{\nu\eta}e^{q^{>}_{\nu\eta}t}+\bar{H}(\lambda^{<}_{1\eta}-t)Q^{<}_{1\eta}e^{q^{<}_{1\eta}t}+\sum_{\nu=1}^{220}H(t-\lambda^{\times}_{1,\nu\eta})\bar{H}(\lambda^{\times}_{2,\nu\eta}-t)Q^{\times}_{\nu\eta}e^{tq^{\times}_{\nu\eta}t}
\end{aligned}\tag{B4}$$

where the corresponding constants are listed below. They are given by

$$\begin{aligned}
\mathcal{T}^{>}_{l;\delta\eta>}&=\sup(\bar{t}_l,\theta^{>}_{\delta\eta}),\quad \mathcal{T}^{<}_{l;1\eta<}=\inf(\bar{t}_l,\theta^{<}_{1\eta}),\\
\mathcal{T}^{>}_{l;i\delta\eta\times}&=\sup(\bar{t}_l,\theta^{\times}_{i,\delta\eta}),\quad \mathcal{T}^{<}_{l;i\delta\eta\times}=\inf(\bar{t}_l,\theta^{\times}_{i,\delta\eta}),
\end{aligned}\tag{B5}$$

and

$$\begin{aligned}
Q^{>}_{\nu=1\to29,\eta}&=F^{>}_{\nu\eta}e^{\gamma_l\bar{t}_l}(D_\eta+f^{>}_{\nu\eta}-\gamma_l)^{-1}, && q^{>}_{\nu\eta}=D_\eta+f^{>}_{\nu\eta}-\gamma_l,\\
& && \lambda^{>}_{\nu\eta}=\mathcal{T}^{>}_{l;\nu\eta>},\\
Q^{>}_{\nu=30\to58,\eta}&=-F^{>}_{(\nu-29)\eta}e^{\gamma_l\bar{t}_l}I(\mathcal{T}^{>}_{l;(\nu-29)\eta>},D_\eta+f^{>}_{(\nu-29)\eta}-\gamma_l), && q^{>}_{\nu\eta}=0,\\
& && \lambda^{>}_{\nu\eta}=\mathcal{T}^{>}_{l;(\nu-29)\eta>},\\
Q^{>}_{\nu=59,\eta}&=F^{<}_{1\eta}e^{\gamma_l\bar{t}_l}H(\theta^{<}_{1\eta}-\bar{t}_l)J(\theta^{<}_{1\eta},\bar{t}_l,D_\eta+f^{<}_{1\eta}-\gamma_l), && q^{>}_{\nu\eta}=0,\\
& && \lambda^{>}_{\nu\eta}=\theta^{<}_{1\eta},\\
Q^{>}_{\nu=60,\eta}&=\sum_{\mu=1}^{29}F^{>}_{\mu\eta}e^{-\gamma_l\bar{t}_l}\bar{H}(\bar{t}_l-\theta^{>}_{\mu\eta})J(\bar{t}_l,\theta^{>}_{\mu\eta},D_\eta+f^{>}_{\mu\eta}+\gamma_l), && q^{>}_{\nu\eta}=0,\\
& && \lambda^{>}_{\nu\eta}=\bar{t}_l,
\end{aligned}\tag{B6}$$

$$\begin{aligned}
&Q^{>}_{\nu=61,\eta}=F^{<}_{1\eta}e^{-\gamma_l\bar{t}_l}I(\mathcal{T}^{<}_{l;1\eta<},D_\eta+f^{<}_{1\eta}+\gamma_l), &&q^{>}_{\nu\eta}=0,\\
& &&\lambda^{>}_{\nu\eta}=\mathcal{T}^{<}_{l;1\eta<},\\
&Q^{>}_{\nu=62\to101,\eta}=F^{\times}_{(\nu-61)\eta}e^{\gamma_l\bar{t}_l}H(\theta^{\times}_{2,(\nu-61)\eta}-\mathcal{T}^{>}_{l;1,(\nu-61)\eta\times}) &&q^{>}_{\nu\eta}=0,\\
&\qquad\times J(\theta^{\times}_{2,(\nu-61)\eta},\mathcal{T}^{>}_{l;1,(\nu-61)\eta\times},D_\eta+f^{\times}_{(\nu-61)\eta}-\gamma_l), &&\lambda^{>}_{\nu\eta}=\theta^{\times}_{2,(\nu-61)\eta},\\
&Q^{>}_{\nu=102\to141,\eta}=F^{\times}_{(\nu-101)\eta}e^{-\gamma_l\bar{t}_l}\overline{H}(\mathcal{T}^{<}_{l;2,(\nu-101)\eta\times}-\theta^{\times}_{1,(\nu-101)\eta}) &&q^{>}_{\nu\eta}=0,\\
&\qquad\times J(\mathcal{T}^{<}_{l;2,(\nu-101)\eta\times},\theta^{\times}_{1,(\nu-101)\eta},D_\eta+f^{\times}_{(\nu-101)\eta}+\gamma_l), &&\lambda^{>}_{\nu\eta}=\mathcal{T}^{<}_{l;2,(\nu-101)\eta\times},\\
&Q^{<}_{\nu=1,\eta}=F^{<}_{1\eta}e^{-\gamma_l t_l}(D_\eta+f^{<}_{1\eta}+\gamma_l)^{-1}, &&q^{<}_{\nu\eta}=D_\eta+f^{<}_{1\eta}+\gamma_l,\\
& &&\lambda^{<}_{\nu\eta}=\mathcal{T}^{<}_{l;1\eta<},\\
&Q^{\times}_{\nu=1,\eta}=F^{<}_{1\eta}e^{\gamma_l\bar{t}_l}H(\theta^{<}_{1\eta}-\overline{t_l})(D_\eta+f^{<}_{1\eta}-\gamma_l)^{-1}, &&q^{\times}_{\nu\eta}=D_\eta+f^{<}_{1\eta}-\gamma_l,\\
& &&\lambda^{\times}_{1,\nu\eta}=\overline{t_l},\\
& &&\lambda^{\times}_{2,\nu\eta}=\theta^{<}_{1\eta},\\
&Q^{\times}_{\nu=2,\eta}=-F^{<}_{1\eta}e^{\gamma_l\bar{t}_l}H(\theta^{<}_{1\eta}-\overline{t_l})I(\overline{t_l},D_\eta+f^{<}_{1\eta}-\gamma_l), &&q^{\times}_{\nu\eta}=0,\\
& &&\lambda^{\times}_{1,\nu\eta}=\overline{t_l},\\
& &&\lambda^{\times}_{2,\nu\eta}=\theta^{<}_{1\eta},\\
&Q^{\times}_{\nu=3\to31,\eta}=F^{>}_{(\nu-2)\eta}e^{-\gamma_l\bar{t}_l}\overline{H}(\overline{t_l}-\theta^{>}_{(\nu-2)\eta})(D_\eta+f^{>}_{(\nu-2)\eta}+\gamma_l)^{-1}, &&q^{\times}_{\nu\eta}=D_\eta+f^{>}_{(\nu-2)\eta}+\gamma_l,\\
& &&\lambda^{\times}_{1,\nu\eta}=\theta^{>}_{(\nu-2)\eta},\\
& &&\lambda^{\times}_{2,\nu\eta}=\overline{t_l},\\
&Q^{\times}_{\nu=32\to60,\eta}=-F^{>}_{(\nu-31)\eta}e^{-\gamma_l\bar{t}_l}\overline{H}(\overline{t_l}-\theta^{>}_{(\nu-31)\eta}) &&q^{\times}_{\nu\eta}=0,\\
&\qquad\times I(\theta^{>}_{(\nu-31)\eta},D_\eta+f^{>}_{(\nu-31)\eta}+\gamma_l), &&\lambda^{\times}_{1,\nu\eta}=\theta^{>}_{(\nu-31)\eta},\\
& &&\lambda^{\times}_{2,\nu\eta}=\overline{t_l},\\
&Q^{\times}_{\nu=61\to100,\eta}=F^{\times}_{(\nu-60)\eta}e^{\gamma_l\bar{t}_l}H(\theta^{\times}_{2,(\nu-60)\eta}-\mathcal{T}^{>}_{l;1(\nu-60)\eta\times}) &&q^{\times}_{\nu\eta}=D_\eta+f^{\times}_{(\nu-60)\eta}-\gamma_l,\\
&\qquad\times(D_\eta+f^{\times}_{(\nu-60)\eta}-\gamma_l)^{-1}, &&\lambda^{\times}_{1,\nu\eta}=\mathcal{T}^{>}_{l;1(\nu-60)\eta\times},\\
& &&\lambda^{\times}_{2,\nu\eta}=\theta^{\times}_{2,(\nu-60)\eta},\\
&Q^{\times}_{\nu=101\to140,\eta}=-F^{\times}_{(\nu-100)\eta}e^{\gamma_l\bar{t}_l}H(\theta^{\times}_{2,(\nu-100)\eta}-\mathcal{T}^{>}_{l;1(\nu-100)\eta\times}) &&q^{\times}_{\nu\eta}=0,\\
&\qquad\times I(\mathcal{T}^{>}_{l;1(\nu-100)\eta\times},D_\eta+f^{\times}_{(\nu-100)\eta}-\gamma_l), &&\lambda^{\times}_{1,\nu\eta}=\mathcal{T}^{>}_{l;1(\nu-100)\eta\times},\\
& &&\lambda^{\times}_{2,\nu\eta}=\theta^{\times}_{2,(\nu-100)\eta}\\
&Q^{\times}_{\nu=141\to180,\eta}=F^{\times}_{(\nu-140)\eta}e^{-\gamma_l\bar{t}_l}\overline{H}(\mathcal{T}^{<}_{l;2(\nu-140)\eta\times}-\theta^{\times}_{1,(\nu-140)\eta}) &&q^{\times}_{\nu\eta}=D_\eta+f^{\times}_{(\nu\text{-}140)\eta}+\gamma_l,\\
&\qquad\times(D_\eta+f^{\times}_{(\nu-140)\eta}+\gamma_l)^{-1}, &&\lambda^{\times}_{1,\nu\eta}=\theta^{\times}_{1,(\nu-140)\eta},\\
& &&\lambda^{\times}_{2,\nu\eta}=\mathcal{T}^{<}_{l;2(\nu-140)\eta\times},\\
&Q^{\times}_{\nu=181\to220,\eta}=-F^{\times}_{(\nu-180)\eta}e^{-\gamma_l\bar{t}_l}\overline{H}(\mathcal{T}^{<}_{l;2(\nu-180)\eta\times}-\theta^{\times}_{1,(\nu-180)\eta}) &&q^{\times}_{\nu\eta}=0,\\
&\qquad\times I(\theta^{\times}_{1,(\nu-180)\eta},D_\eta+f^{\times}_{(\nu-180)\eta}+\gamma_l), &&\lambda^{\times}_{1,\nu\eta}=\theta^{\times}_{1,(\nu-180)\eta},\\
& &&\lambda^{\times}_{2,\nu\eta}=\mathcal{T}^{<}_{l;2(\nu-180)\eta\times}.
\end{aligned}$$

[1] C. L. Tang and C. Flytzanis, Phys. Rev. B **4**, 2520 (1971).

[2] Y. R. Shen, *The Principles of Nonlinear Optics* (Wiley-Interscience, New York, 1984).

[3] S. R. Meech, in *Advances in Multiphoton Processes and Spectroscopy*, edited by S. H. Lin, A. A. Villaeys, and Y. Fujimura (World Scientific, Singapore, 1993), Vol. 8, p. 281.

[4] S. H. Lin and A. A. Villaeys, Phys. Rev. A **50**, 5134 (1994).

[5] J. C. Vallet, A. J. Boeglin, J. P. Lavoine, and A. A. Villaeys, Chem. Phys. Lett. **241**, 203 (1995).

[6] J. C. Vallet, A. J. Boeglin, J. P. Lavoine, and A. A. Villaeys, Phys. Rev. A **53**, 4508 (1996).

[7] T. F. Heinz, C. K. Chen, D. Ricard, and Y. R. Shen, Phys. Rev. Lett. **48**, 478 (1982).

[8] S. H. Lin, R. G. Alden, A. A. Villaeys, and V. Pflumio, Phys. Rev. A **48**, 3137 (1993).

[9] N. Akamatsu, K. Domen, C. Hirose, T. Onishi, H. Shimizu, and K. Matsutani, Chem. Phys. Lett. **181**, 175 (1991).

[10] C. Hirose, H. Yamamoto, N. Akamatsu, and K. Domen, J. Phys. Chem. **97**, 10 064 (1993).

[11] N. Akamatsu, K. Domen, and C. Hirose, J. Phys. Chem. **97**, 10 070 (1993).

[12] V. Pflumio, J. C. Vallet, A. A. Villaeys, and J. P. Lavoine, Phys. Rev. A **51**, 3174 (1995).

[13] S. R. Hatch, R. S. Polizzotti, S. Dougal, and P. Rabinowitz, Chem. Phys. Lett. **196**, 97 (1990).

[14] P. Guyot-Sionnest, Phys. Rev. Lett. **67**, 2323 (1991).

[15] P. Guyot-Sionnest, P. Dumas, Y. J. Chabal, and G. S. Higashi, Phys. Rev. Lett. **64**, 2156 (1990).

[16] R. P. Chin, X. Blase, Y. R. Shen, and S. G. Louie, Europhys. Lett. **30**, 399 (1995).

[17] Y-Chieh Sun, H. Gai, and G. A. Vith, J. Chem. Phys. **100**, 3247 (1994).

[18] A. L. Harris, L. Rothberg, L. H. Dubois, N. J. Levinos, and L. Dhar, Phys. Rev. Lett. **64**, 2086 (1990).

[19] A. L. Harris, L. Rothberg, L. Dhar, N. J. Levinos, and L. H. Dubois, J. Chem. Phys. **94**, 2438 (1991).

[20] A. L. Harris and L. Rothberg, J. Chem. Phys. **94**, 2449 (1991).

[21] T. Kato, M. Hayashi, A. A. Villaeys, and S. H. Lin, Phys. Rev. A **56**, 980 (1997).

[22] T. Yajima and H. Souma, Phys. Rev. A **17**, 309 (1978).

[23] T. Yajima, H. Souma, and Y. Ishida, Phys. Rev. A **17**, 324 (1978).

[24] R. W. Boyd and S. Mukamel, Phys. Rev. A **29**, 1973 (1984).

[25] G. Placzek, in *Molecular Vibrations*, edited by E. B. Wilson, J. C. Decius, and P. C. Cross (Dover, New York, 1995).

[26] S. Mukamel, *Principles of Nonlinear Optical Spectroscopy* (Oxford University Press, New York, 1995).

[27] C. M. Laursen, E. Christoffersen, and G. D. Billing, Chem. Phys. Lett. **290**, 275 (1998).

[28] L. Chen, R. Wu, N. Kioussis, and Q. Zhang, Chem. Phys. Lett. **290**, 255 (1998).

[29] P. Guyot-Sionnest, P. Dumas, and Y. J. Chabal, J. Electron. Spectrosc. Relat. Phenom. **54/57**, 27 (1990).

[30] A. A. Villaeys, V. Pflumio, and S. H. Lin, Phys. Rev. A **49**, 4996 (1994).